AIMS Mathematics

https://www.aimspress.com/journal/Math

AIMS Mathematics, 11(1): 1820–1856.
DOI: 10.3934/math.2026076
Received: 23 October 2025
Revised: 16 December 2025
Accepted: 08 January 2026
Published: 20 January 2026

Research article

An efficient numerical method to solve 2D parabolic singularly perturbed coupled systems of convection-diffusion type with multi-parameters on a Bakhvalov–Shishkin mesh

Ram Shiromani[1] **and Carmelo Clavero**[2,*]

[1] Symbiosis Centre for Information Technology, Symbiosis International (Deemed University), Pune, India

[2] Department of Applied Mathematics, IUMA, University of Zaragoza, Zaragoza, Spain

* **Correspondence:** Email: clavero@unizar.es.

Abstract: This study addresses the efficient solution of a class of 2D parabolic singularly perturbed weakly coupled systems of convection-diffusion type. In the model problem, small positive parameters appear in both the diffusion and the convection terms. We assume that the diffusion parameters can be distinct, but the convection parameter remains the same for both equations. Then, for sufficiently small values of the parameters, overlapping boundary layers appear on the boundary of the spatial domain. To solve the problem, a numerical method is employed that combines the implicit Euler scheme, defined on a uniform mesh, with the upwind scheme for spatial discretization. Then, if the spatial discretization is carried out on an adequate nonuniform Bakhvalov–Shishkin (BS) mesh, the fully discrete scheme attains uniform convergence, with respect to all perturbation parameters; moreover, it has first-order accuracy in both temporal and spatial variables. Note that the construction of the BS mesh depends on the value and the ratio between the diffusion and the convection parameters, and special generating functions are needed to construct them. Numerical experiments illustrating the performance of the algorithm for some test problems are showed, which corroborate the uniform convergence of the method in agreement with the theoretical results.

Keywords: 2D parabolic weakly coupled systems; diffusion and convection parameters; Bakhvalov–Shishkin meshes; uniform convergence
Mathematics Subject Classification: 35B25, 35J40, 35J25, 65N06, 65N15, 65N12, 65N50

1. Introduction

The present work studies the numerical treatment of a 2D singularly perturbed parabolic system of weakly coupled equations. The governing model can be expressed in the form

$$\mathcal{L}_{\varepsilon,\mu}\mathbf{z} \equiv \frac{\partial z}{\partial t} - \boldsymbol{\varepsilon}\Delta z + \boldsymbol{\mu}\sum_{i=1}^{2}\boldsymbol{A}_i(x_1,x_2,t)\frac{\partial z}{\partial x_i} + \mathbf{B}(x_1,x_2,t)\,z = \mathbf{f}(x_1,x_2,t), \quad (x_1,x_2,t)\in Q := \Omega\times(0,T], \tag{1.1a}$$

with boundary and initial conditions given by

$$z(x_1,x_2,t) = \boldsymbol{q}(x_1,x_2,t), \quad (x_1,x_2,t)\in\partial\Omega\times[0,T], \qquad z(x_1,x_2,0) = \boldsymbol{\psi}(x_1,x_2,0), \quad (x_1,x_2)\in\Omega, \tag{1.1b}$$

where the spatial domain is $\Omega = \Omega_{x_1}\times\Omega_{x_2}$, being $\Omega_{x_1} = \Omega_{x_2} = (0,1)$. We denote spatial domain's boundary edges as $\Gamma = \Gamma_l\cup\Gamma_b\cup\Gamma_r\cup\Gamma_t$, where

$$\partial\Omega = \begin{cases} \Gamma_l = \{(0,x_2)\,|\,x_2\in[0,1]\}, & \Gamma_b = \{(x_1,0)\,|\,x_1\in[0,1]\},\\ \Gamma_r = \{(1,x_2)\,|\,x_2\in[0,1]\}, & \Gamma_t = \{(x_1,1)\,|\,x_1\in[0,1]\}. \end{cases}$$

Since $z = \boldsymbol{q}$ on $\partial\Omega$ by (1.1), let $\boldsymbol{q}_k := \boldsymbol{q}|_{\Gamma_k}$ for $k\in\{l,b,r,t\}$, where $\Gamma_l,\Gamma_b,\Gamma_r,\Gamma_t$ represent the boundary portions on the left, bottom, right, and top sides of the domain, respectively.

The convection matrices are denoted by $\boldsymbol{A}_i = \mathrm{diag}(a^i_{11},a^i_{22})$, $i = 1,2$ and the reaction matrix by $\mathbf{B} = (b_{kl})_{2\times2}$, respectively. Furthermore, the differential operator, the diffusion and convection term, the source term, and the boundary data are specified as

$$\begin{aligned}&\mathcal{L}_{\varepsilon,\mu} = (\mathcal{L}^1_{\varepsilon_1,\mu},\mathcal{L}^2_{\varepsilon_2,\mu})^T, \boldsymbol{\varepsilon} = (\varepsilon_1,\varepsilon_2)^T, \boldsymbol{\mu} = (\mu,\mu)^T, \mathbf{z} = (z_1,z_2)^T,\\ &\mathbf{f} = (f_1,f_2)^T, \mathbf{q}_k = (q_{k1},q_{k2})^T,\ k = 1,\dots,4.\end{aligned}$$

We consider the perturbation parameters ε_1, ε_2 to satisfy $0<\varepsilon_1\le\varepsilon_2\ll 1$ and $0<\mu\ll 1$. Additionally, the coefficients of reaction and the convection matrices satisfy the conditions

$$\begin{cases} a^i_{kk}\ge\vartheta>0,\ b_{kk}\ge\beta>0,\ \ k,i = 1,2,\ \ b_{kk}>|b_{kl}|,\ \ b_{kl}\le 0,\ \ k\ne l,\ l,k = 1,2,\\ \Lambda = \min\limits_{k,l}\left\{\dfrac{b_{kk}-b_{kl}}{2a^i_{11}},\dfrac{b_{kk}-b_{kl}}{2a^i_{22}}\right\},\ \text{ for } k,l,i = 1,2,\ k\ne l, \end{cases} \tag{1.2}$$

for some positive constants ϑ and β. Finally, the entries of $\mathbf{A}_i$, $\mathbf{B}$, and $\mathbf{f}$ are sufficiently smooth functions on the domain Ω, and the boundary data satisfy $\mathbf{q}_k\in C^{3,\gamma}(\Gamma_k)$ for $k\in\{l,b,r,t\}$, with $\gamma\in(0,1]$. Furthermore, these functions are assumed to satisfy the necessary compatibility constraints to ensure the existence of a classical solution $\mathbf{z}$ to the continuous model, such that $\mathbf{z}\in C^{3,\gamma}(\overline{\Omega})$.

Coupled singularly perturbed systems are interesting problems in the applied mathematics area, because they are good mathematical models of many physical phenomena in different areas such as transport and dispersion of pollutants in a fluid or porous media, simulation of oil and gas reservoirs, bio-fluids mechanics, magnetohydrodynamic flow, population dynamics, control theory, quantum mechanics, or elasticity (see, by instance, the works of Epstein et al [12], Gill-Robertson [14] and Kan-On-Miura [18], and the books of Pao [27] and Murray [23]). Recent advancements in meshfree and hybrid numerical methods have shown strong potential for solving complex multi-dimensional problems. Peng et al. [28] demonstrated the efficiency of a hybrid reproducing kernel particle method for 3D elasticity, while Cheng et al. [4] proposed a hybrid interpolating element-free Galerkin method that effectively handles convection-dominated diffusion problems. For diffusion-based applications, Zheng and Cheng [36] introduced an improved element-free Galerkin method that enhances accuracy in drug-release modeling. These works collectively highlight the effectiveness of meshfree hybrid approaches as reliable alternatives to traditional numerical schemes.

In particular, magnetohydrodynamic (MHD) flow problems serve as a representative example where such systems naturally appear. A simplified steady 2D linearized model, coupling a velocity-like scalar u with a magnetic-like scalar b, can be formulated as

$$\begin{cases} -\varepsilon_u \Delta u + \mathbf{a} \cdot \nabla u + \alpha\, u + \delta\, \beta\, b = f_u(x, y), \\ -\varepsilon_b \Delta b + \mathbf{a} \cdot \nabla b + \gamma\, b + \delta\, \theta\, u = f_b(x, y), \end{cases} \tag{1.3}$$

subject to suitable boundary conditions.
Here, the model components can be interpreted as follows:

- u: velocity perturbation (streamwise component),
- b: magnetic field perturbation (or scalar potential),
- $\varepsilon_u = \nu$: kinematic viscosity,
- $\varepsilon_b = \eta$: magnetic diffusivity (with both $\nu, \eta \ll 1$, sharp boundary layers such as Hartmann layers may form),
- $\mathbf{a}$: mean flow advection velocity, and
- $\delta\beta$, $\delta\theta$: weak Lorentz force and induction coupling terms (lower-order contributions).

The parameter δ characterizes the degree of coupling. When $\delta \ll 1$, the Lorentz-force/induction feedback is relatively weak compared to the dominant advective and diffusive dynamics, thus fitting into the framework of weakly coupled singular perturbations.

It is well known that the solution of singularly perturbed problems (SPPs) is characterized by the presence of boundary layers and, in certain cases, internal layers, which can be of different types (regular, parabolic, internal, ...). Then, the use of classical numerical techniques, defined on uniform meshes, is not adequate because the numerical solution degrades when the parameters are small unless the step size of the grid is very small (depending on parameter choice), which is not computationally efficient. Therefore, to develop efficient methods that yield accurate solutions for all parameters (i.e., uniformly convergent methods), it becomes essential to design numerical methods tailored to the specific class of problems under consideration.

A special type of SPPs appears when small parameters are present for both the diffusion and the convection terms; this type of problem has had a lot of interest in the last years for linear and nonlinear singularly perturbed problems (see, for instance, the works of Avijit-Natesan [2], Clavero-Jorge [7], Govindarao et al [15, 16], Jha-Kadalabajoo [17], O'Riordan et al [25, 26] and Priyadarshana-Mohapatra [29–31]). Inside this type of problem, singularly perturbed systems are a particular case; their theoretical analysis is more difficult due the complex structure of the boundary layers (overlapping boundary layers) that appear in the solution of the continuous problem. In the literature, there exits many works where both elliptic and parabolic coupled systems are considered; nevertheless, the most canalized problem is one where small parameters appear only in the diffusion term (see, for instance, the works of Cen [3], Clavero-Jorge [5,6], Kumar-Kumar [19], Liu et al [22], Priyadharshini et al [32] and Singh-Natesan [33–35]). A different and more difficult case is one where in the equations of the coupled system, small parameters are present in both the diffusion and the convection terms. For instance, in [1], a 1D weakly coupled parabolic system of convection-diffusion type was introduced. In the works by Clavero-Shiromani [10, 11] and Clavero et al [8, 9], a 2D weakly-coupled elliptic system was studied for different cases. In [24], a 1D weakly coupled elliptic system was considered, for which the diffusion parameters at each equation are different and the convection parameters are identical in both equations. This work uses similar methodologies to those in [10], where a 2D elliptic system with different parameters in the diffusion and equal convection parameters was studied. In that work, it was proved that the structure of overlapping boundary layers at the inflow and outflow boundaries of the domain is complex. The use of Shishkin meshes is the most standard in the literature; the numerical method gives an almost first-order uniformly convergent method due the presence of a logarithmic factor, which is associated to the definition of the Shishkin mesh. To improve this order of uniform convergence and to eliminate the logarithmic factor, here we consider a different type of nonuniform mesh, the BS mesh, which is also very popular in the context of the numerical resolution of singularly perturbed problems. The construction of this is considerably more difficult than the Shishkin mesh, and it is not a piecewise uniform mesh; nevertheless, its use gives better numerical results without increasing the computational cost of the numerical method. Therefore, we aim to highlight the numerical advantages of using this mesh in comparison with the standard Shishkin mesh.

The structure of the paper is as follows. In Section 2, we analyze the asymptotic behavior of the exact solution and derive appropriate estimates for its partial derivatives, which depend on the value and the ratio between the diffusion and convection parameters; these findings provide a foundation for the later study of uniform convergence. Section 3 focuses on the development of the fully discrete scheme, including the definition of meshes that reflect the asymptotic characteristics of the continuous problem. In Section 4, we prove the uniform convergence of the fully discrete scheme, establishing first-order accuracy with respect to both temporal and spatial discretization. Section 5 presents numerical experiments on representative test problems of type (1.1), validating the theoretical results and confirming the method's uniform convergence. Finally, Section 6 concludes the paper with a summary of the main findings.

Henceforth, we denote by $\|\cdot\|$ the continuous maximum norm. For a vector-valued function $\boldsymbol{\Psi} = (\Psi_1, \Psi_2)^T$, we define $|\boldsymbol{\Psi}| = (|\Psi_1|, |\Psi_2|)^T$. Throughout the subsequent analysis, C represents a generic positive constant that is independent of the diffusion parameters ε_1 and ε_2, the convection parameter μ, and the discretization parameters N and M.

2. Asymptotic analysis of the exact solution to the continuous problem

This section investigates the asymptotic properties of the exact solution, along with its decomposition into regular and singular parts, and establishes estimates for its partial derivatives with respect to the diffusion and convection parameters. The approach adopted here is based on the framework and techniques introduced in [10].

Lemma 2.1 (Maximum principle)**.** *Consider the differential operator $\mathcal{L}_{\varepsilon,\mu}$ defined in (1.1), and suppose that condition (1.2) is satisfied. If $\mathfrak{v}(x_1, x_2, t) \geq \mathbf{0}$ on $\partial\Omega\times[0, T]\cup\Omega\times\{0\}$ and $\mathcal{L}_{\varepsilon,\mu}\mathfrak{v}(x_1, x_2, t) \geq \mathbf{0}$ for all $(x_1, x_2, t) \in Q$, then it follows that $\mathfrak{v}(x_1, x_2, t) \geq \mathbf{0}$ for all $(x_1, x_2, t) \in \overline{Q}$.*

Lemma 2.2 (Stability result). *Let* $\mathfrak{v} \in C^{4,2}(\overline{Q})$*; then, it holds that*

$$|\mathfrak{v}(x_1, x_2, t)| \leq \frac{1}{\vartheta}\|\mathcal{L}_{\varepsilon,\mu}\mathfrak{v}\| + \max\{\|\mathfrak{v}\|_{\partial\Omega\times[0,T]}, \|\mathfrak{v}\|_{\Omega\times\{0\}}\},$$

where ϑ *is the constant defined in (1.2).*

Theorem 2.3. *Let* z *denote the exact solution of (1.1). Then, on the domain* $\overline{Q}$*, the derivatives of* z *admit the following estimates:*

$$\left|\frac{\partial^{(l_1+l_2+l_3)}z}{\partial {x_1}^{l_1}\partial {x_2}^{l_2}\partial t^{l_3}}\right| \leq C(\boldsymbol{\varepsilon})^{(-l_1-l_2)/2}\left\{1 + \left(\frac{\boldsymbol{\mu}}{\sqrt{\boldsymbol{\varepsilon}}}\right)^{(l_1+l_2)}\right\},\ 1 \leq l_1 + l_2 + 2l_3 \leq 2, \tag{2.1a}$$

$$\left|\frac{\partial^{(l_1+l_2+l_3)}z_1}{\partial {x_1}^{l_1}\partial {x_2}^{l_2}\partial t^{l_3}}\right| \leq C(\varepsilon_1)^{(-l_1-l_2)/2}\left\{1 + \left(\frac{\mu}{\sqrt{\varepsilon_1}}\right)^{(l_1+l_2)}\right\} + C\varepsilon_1^{2-l_1-l_2},\ 3 \leq l_1 + l_2 + 2l_3 \leq 4, \tag{2.1b}$$

$$\left|\frac{\partial^{(l_1+l_2+l_3)}z_2}{\partial {x_1}^{l_1}\partial {x_2}^{l_2}\partial t^{l_3}}\right| \leq C(\varepsilon_2)^{(-l_1-l_2)/2}\left\{1 + \left(\frac{\mu}{\sqrt{\varepsilon_2}}\right)^{(l_1+l_2)}\right\} + C\varepsilon_1^{1-(l_1+l_2)/2}\varepsilon_2^{-1},\ 3 \leq l_1 + l_2 + 2l_3 \leq 4. \tag{2.1c}$$

Proof. This result follows directly from [20]. □

Following to [10], the exact solution $\mathbf{z}$ of problem (1.1) is decomposed into its smooth function $\mathbf{r}$, boundary layer $\mathbf{w}$, and corner layer components $\mathbf{s}$. Furthermore, the smooth component is characterized as the solution of the following problem:

$$\mathcal{L}_{\varepsilon,\mu}\mathbf{r}(x_1, x_2, t) = \mathbf{f}, \quad \forall(x_1, x_2, t) \in Q, \tag{2.2a}$$

with boundary and initial conditions given by

$$\mathbf{r}(x_1, x_2, t) = \varphi(x_1, x_2, t), \quad \forall(x_1, x_2, t) \in \partial\Omega \times [0, T], \quad \mathbf{r}(x_1, x_2, 0) = \boldsymbol{\psi}(x_1, x_2), \quad \forall(x_1, x_2) \in \Omega, \tag{2.2b}$$

where $\boldsymbol{r} = \varphi$ are appropriate functions (see the posterior analysis) for the regular component, and we denote by φ_i the restriction of φ onto Γ_i, $i = l, b, r, t$.

The boundary layer component is refined into $\mathbf{w}_k$ for $k \in \{l, r, b, t\}$, each of which is determined as the solution of

$$\mathcal{L}_{\varepsilon,\mu}\mathbf{w}_k(x_1, x_2, t) = \mathbf{0},\ k = l, r, b, t, \quad \forall(x_1, x_2, t) \in Q, \tag{2.3a}$$

with boundary and initial conditions given by

$$\mathbf{w}_k(x_1, x_2, t) = (\mathbf{z} - \mathbf{r})(x_1, x_2, t),\ \forall(x_1, x_2, t) \in \Gamma_k \times [0, T], \quad \mathbf{w}_k(x_1, x_2, t) = 0,\ \forall(x_1, x_2, t) \in (\Gamma\backslash\Gamma_k) \times [0, T]. \tag{2.3b}$$

Finally, the corner layer component is decomposed into $\mathbf{s}_k$ for $k \in \{lb, br, rt, lt\}$, each governed by:

$$\mathcal{L}_{\varepsilon,\mu}\mathbf{s}_k(x_1, x_2, t) = \mathbf{0},\ k = k_1k_2,\ (k_1, k_2) \in \{(l, b),\ (b, r),\ (r, t),\ (l, t)\}, \quad \forall(x_1, x_2, t) \in Q, \tag{2.4a}$$

with boundary and initial conditions given by

$$\mathbf{s}_k(x_1, x_2, t) = -\mathbf{w}_{k_1}(x_1, x_2, t),\ \forall(x_1, x_2, t) \in \Gamma_{k_1} \times [0, T],\ \mathbf{s}_k(x_1, x_2, t) = -\mathbf{w}_{k_2}(x_1, x_2, t),\ \forall(x_1, x_2, t) \in \Gamma_{k_2} \times [0, T], \tag{2.4b}$$

$$\mathbf{s}_k(x_1, x_2, t) = 0,\ \forall(x_1, x_2, t) \in (\Gamma\backslash\{\Gamma_{k_1} \cup \Gamma_{k_2}\}) \times [0, T]. \tag{2.4c}$$

In [10], the following results were proved.

Theorem 2.4. *Let $\boldsymbol{r}$, where $\boldsymbol{r} = (r_1, r_2)^T$, satisfy the problem (2.2). Then,*
• *If $\vartheta\mu^2 \le \Lambda\varepsilon_1$ holds, we have*

$$\left\|\frac{\partial^{l_1+l_2+l_3} r_1}{\partial x_1{}^{l_1}\partial x_2{}^{l_2}\partial t^{l_3}}\right\| \le C, \quad 0 \le l_1 + l_2 + 2l_3 \le 2, \ \left\|\frac{\partial^{l_1+l_2+l_3} r_1}{\partial x_1{}^{l_1}\partial x_2{}^{l_2}\partial t^{l_3}}\right\| \le C\varepsilon_1^{-1/2}, \ l_1 + l_2 + 2l_3 = 3, \tag{2.5a}$$

$$\left\|\frac{\partial^{l_1+l_2+l_3} r_2}{\partial x_1{}^{l_1}\partial x_2{}^{l_2}\partial t^{l_3}}\right\| \le C, \quad 0 \le l_1 + l_2 + 2l_3 \le 3. \tag{2.5b}$$

• *If $\vartheta\mu^2 \ge \Lambda\varepsilon_2$ holds, we have*

$$\left\|\frac{\partial^{l_1+l_2+l_3} \boldsymbol{r}}{\partial x_1{}^{l_1}\partial x_2{}^{l_2}\partial t^{l_3}}\right\| \le C, \ 0 \le l_1 + l_2 + 2l_3 \le 2, \ \left\|\frac{\partial^{l_1+l_2+l_3} r_1}{\partial x_1{}^{l_1}\partial x_2{}^{l_2}\partial t^{l_3}}\right\| \le C\varepsilon_1^{-1}, \ l_1 + l_2 + 2l_3 = 3, \tag{2.6a}$$

$$\left\|\frac{\partial^{l_1+l_2+l_3} r_2}{\partial x_1{}^{l_1}\partial x_2{}^{l_2}\partial t^{l_3}}\right\| \le C, \ l_1 + l_2 + 2l_3 = 3. \tag{2.6b}$$

• *Finally, if $\Lambda\varepsilon_1 < \vartheta\mu^2 < \Lambda\varepsilon_2$ holds, we have*

$$\left\|\frac{\partial^{l_1+l_2+l_3} \boldsymbol{r}}{\partial x_1{}^{l_1}\partial x_2{}^{l_2}\partial t^{l_3}}\right\| \le C, \ 0 \le l_1 + l_2 + 2l_3 \le 2, \ \left\|\frac{\partial^{l_1+l_2+l_3} r_1}{\partial x_1{}^{l_1}\partial x_2{}^{l_2}\partial t^{l_3}}\right\| \le C\varepsilon_1^{-1}, \ l_1 + l_2 + 2l_3 = 3, \tag{2.7a}$$

$$\left\|\frac{\partial^{l_1+l_2+l_3} r_2}{\partial x_1{}^{l_1}\partial x_2{}^{l_2} t^{l_3}}\right\| \le C\varepsilon_2^{-1/2}, \ l_1 + l_2 + 2l_3 = 3. \tag{2.7b}$$

To establish the asymptotic behavior of the layer functions, we use the funtions $\mathcal{G}_i^l(x_1)$, $\mathcal{G}_i^r(x_2)$, $i = 1, 2$, defined by

$$\mathcal{G}_1^l(x_1) = \begin{cases} e^{-\theta_1 x_1}, \ \vartheta\mu^2 \le \Lambda\varepsilon_1, \\ e^{-\kappa x_1}, \ \vartheta\mu^2 \ge \Lambda\varepsilon_2, \\ e^{-\kappa x_1}, \ \Lambda\varepsilon_1 < \vartheta\mu^2 < \Lambda\varepsilon_2, \end{cases} \qquad \mathcal{G}_1^r(x_1) = \begin{cases} e^{-\theta_1(1-x_1)}, \ \vartheta\mu^2 \le \Lambda\varepsilon_1, \\ e^{-\lambda_1(1-x_1)}, \ \vartheta\mu^2 \ge \Lambda\varepsilon_2, \\ e^{-\lambda_1(1-x_1)}, \ \Lambda\varepsilon_1 < \vartheta\mu^2 < \Lambda\varepsilon_2, \end{cases} \tag{2.8a}$$

$$\mathcal{G}_2^l(x_1) = \begin{cases} e^{-\theta_2 x_1}, \ \vartheta\mu^2 \le \Lambda\varepsilon_1, \\ e^{-\kappa x_1}, \ \vartheta\mu^2 \ge \Lambda\varepsilon_2, \\ e^{-\theta_2 x_1}, \ \Lambda\varepsilon_1 < \vartheta\mu^2 < \Lambda\varepsilon_2, \end{cases} \qquad \mathcal{G}_2^r(x_1) = \begin{cases} e^{-\theta_2(1-x_1)}, \ \vartheta\mu^2 \le \Lambda\varepsilon_1, \\ e^{-\lambda_2(1-x_1)}, \ \vartheta\mu^2 \ge \Lambda\varepsilon_2, \\ e^{-\lambda_2(1-x_1)}, \ \Lambda\varepsilon_1 < \vartheta\mu^2 < \Lambda\varepsilon_2, \end{cases} \tag{2.8b}$$

where $\theta_i = \sqrt{\dfrac{\Lambda\vartheta}{\varepsilon_i}}$, $\lambda_i = \dfrac{\vartheta\mu}{\varepsilon_i}$, and $\kappa = \dfrac{\Lambda}{2\mu}$, for $i = 1, 2$.

Analogously, we can define $\mathcal{G}_i^l(x_2)$, $\mathcal{G}_i^r(x_2)$, $\mathcal{G}_i^b(x_1)$, $\mathcal{G}_i^t(x_1)$, $\mathcal{G}_i^b(x_2)$, $\mathcal{G}_i^t(x_2)$, $i = 1, 2$, for the left, right, top, and bottom boundaries.

Theorem 2.5. *Consider $\mathbf{w}_k$, $k \in \{l, r, b, t\}$, with $\mathbf{w}_k = (w_{k_1}, w_{k_2})^T$, which are solutions to problem (2.3). Then,*
• *If $\vartheta\mu^2 \le \Lambda\varepsilon_1$ holds, we have*

$$|w_{l_1}| \le C\mathcal{G}_2^l(x_1), \ |w_{l_2}| \le C\mathcal{G}_2^l(x_1), \ |w_{b_1}| \le C\mathcal{G}_2^b(x_2), \ |w_{b_2}| \le C\mathcal{G}_2^b(x_2),$$
$$\left|\frac{\partial^{i+j+k} w_{l_1}}{\partial x_1{}^i\partial x_2{}^j\partial t^k}\right| \le C(\varepsilon_1^{-i/2}\mathcal{G}_1^l(x_1) + \varepsilon_2^{-i/2}\mathcal{G}_2^l(x_1)),$$

$$\left|\frac{\partial^{i+j+k}w_{b_1}}{\partial x_1{}^i\partial x_2{}^j\partial t^k}\right| \le C(\varepsilon_1^{-j/2}\mathcal{G}_1^b(x_2)+\varepsilon_2^{-j/2}\mathcal{G}_2^b(x_2)),\ 1\le i+j+2k\le 3,$$
$$\left|\frac{\partial^{i+j+k}w_{l_2}}{\partial x_1{}^i\partial x_2{}^j\partial t^k}\right| \le C\varepsilon_2^{-i/2}\mathcal{G}_2^l(x_1),\ 1\le i+j+2k\le 2,$$
$$\left|\frac{\partial^{i+j+k}w_{l_2}}{\partial x_1{}^i\partial x_2{}^j\partial t^k}\right| \le C\varepsilon_2^{-1}(\varepsilon_1^{-1/2}\mathcal{G}_1^l(x_1)+\varepsilon_2^{-1/2}\mathcal{G}_2^l(x_1)),\ i+j+2k=3,$$
$$\left|\frac{\partial^{i+j+k}w_{b_2}}{\partial x_1{}^i\partial x_2{}^j\partial t^k}\right| \le C\varepsilon_2^{-j/2}\mathcal{G}_2^b(x_2), 1\le i+j+2k\le 2,$$
$$\left|\frac{\partial^{i+j+k}w_{b_2}}{\partial x_1{}^i\partial x_2{}^j\partial t^k}\right| \le C\varepsilon_2^{-1}(\varepsilon_1^{-1/2}\mathcal{G}_1^b(x_2)+\varepsilon_2^{-1/2}\mathcal{G}_2^b(x_2)),\ i+j+2k=3,$$

$$|w_{r_1}|\le C\mathcal{G}_2^r(x_1),\ |w_{r_2}|\le C\mathcal{G}_2^r(x_1),\ \ |w_{t_1}|\le C\mathcal{G}_2^t(x_2),\ |w_{t_2}|\le C\mathcal{G}_2^l(x_2),$$
$$\left|\frac{\partial^{i+j+k}w_{r_1}}{\partial x_1{}^i\partial x_2{}^j\partial t^k}\right| \le C(\varepsilon_1^{-i/2}\mathcal{G}_1^r(x_1)+\varepsilon_2^{-i/2}\mathcal{G}_2^r(x_1)),$$
$$\left|\frac{\partial^{i+j+k}w_{t_1}}{\partial x_1{}^i\partial x_2{}^j\partial t^k}\right| \le C(\varepsilon_1^{-j/2}\mathcal{G}_1^t(x_2)+\varepsilon_2^{-j/2}\mathcal{G}_2^t(x_2)),\ 1\le i+j+2k\le 3,$$
$$\left|\frac{\partial^{i+j+k}w_{r_2}}{\partial x_1{}^i\partial x_2{}^j\partial t^k}\right| \le C\varepsilon_2^{-i/2}\mathcal{G}_2^r(x_1),\ 1\le i+j+2k\le 2,$$
$$\left|\frac{\partial^{i+j+k}w_{r_2}}{\partial x_1{}^i\partial x_2{}^j\partial t^k}\right| \le C\varepsilon_2^{-1}(\varepsilon_1^{-1/2}\mathcal{G}_1^r(x_1)+\varepsilon_2^{-1/2}\mathcal{G}_2^r(x_1)),\ i+j+2k=3,$$
$$\left|\frac{\partial^{i+j+k}w_{t_2}}{\partial x_1{}^i\partial x_2{}^j\partial t^k}\right| \le C\varepsilon_2^{-j/2}\mathcal{G}_2^t(x_2), 1\le i+j+2k\le 2,$$
$$\left|\frac{\partial^{i+j+k}w_{t_2}}{\partial x_1{}^i\partial x_2{}^j\partial t^k}\right| \le C\varepsilon_2^{-1}(\varepsilon_1^{-1/2}\mathcal{G}_1^t(x_2)+\varepsilon_2^{-1/2}\mathcal{G}_2^t(x_2))\,i+j+2k=3.$$

• *If* $\vartheta\mu^2\ge\Lambda\varepsilon_2$ *holds, we have*

$$|w_{l_1}|\le C\mathcal{G}_2^l(x_1),\ |w_{l_2}|\le C\mathcal{G}_2^l(x_1),\ \ |w_{b_1}|\le C\mathcal{G}_2^b(x_2),\ |w_{b_2}|\le C\mathcal{G}_2^b(x_2),$$
$$\left|\frac{\partial^{i+j+k}w_{l_1}}{\partial x_1{}^i\partial x_2{}^j\partial t^k}\right| \le C\mu^i(\varepsilon_1^{-i}\mathcal{G}_1^l(x_1)+\varepsilon_2^{-i}\mathcal{G}_2^l(x_1)),\ \left|\frac{\partial^{i+j+k}w_{b_1}}{\partial x_1{}^i\partial x_2{}^j\partial t^k}\right| \le C\mu^j(\varepsilon_1^{-j}\mathcal{G}_1^b(x_2)+\varepsilon_2^{-j}\mathcal{G}_2^b(x_2)),\ 1\le i+j+2k\le 3,$$
$$\left|\frac{\partial^{i+j+k}w_{l_2}}{\partial x_1{}^i\partial x_2{}^j\partial t^k}\right| \le C\mu^i\varepsilon_2^{-i}\mathcal{G}_2^l(x_1),\ 1\le i+j+2k\le 2,\ \left|\frac{\partial^{i+j+k}w_{l_2}}{\partial x_1{}^i\partial x_2{}^j\partial t^k}\right| \le C\Big(\frac{\mu^3}{\varepsilon_1\varepsilon_2^2}\mathcal{G}_1^l(x_1)+\frac{\mu^3}{\varepsilon_2^3}\mathcal{G}_2^l(x_1)\Big),\ i+j+2k=3,$$
$$\left|\frac{\partial^{i+j+k}w_{b_2}}{\partial x_1{}^i\partial x_2{}^j\partial t^k}\right| \le C\mu^j\varepsilon_2^{-j}\mathcal{G}_2^b(x_2),\ 1\le i+j+2k\le 2,\ \left|\frac{\partial^{i+j+k}w_{b_2}}{\partial x_1{}^i\partial x_2{}^j\partial t^k}\right| \le C\Big(\frac{\mu^3}{\varepsilon_1\varepsilon_2^2}\mathcal{G}_1^b(x_2)+\frac{\mu^3}{\varepsilon_2^3}\mathcal{G}_2^b(x_2)\Big),\ i+j+2k=3,$$
$$|w_{r_1}|\le C,\ |w_{r_2}|\le C,\ \ |w_{t_1}|\le C,\ |w_{t_2}|\le C,$$
$$\left|\frac{\partial^{i+j+k}w_{r_1}}{\partial x_1{}^i\partial x_2{}^j\partial t^k}\right| \le C\mu^{-i},\ 1\le i+j+2k\le 2,\ \left|\frac{\partial^{i+j+k}w_{r_1}}{\partial x_1{}^i\partial x_2{}^j\partial t^k}\right| \le C\mu^{-3}+C\varepsilon_1^{-1},\ i+j+2k=3,$$
$$\left|\frac{\partial^{i+j+k}w_{r_2}}{\partial x_1{}^i\partial x_2{}^j\partial t^k}\right| \le C\mu^{-i},\ 1\le i+j+2k\le 3,\ \left|\frac{\partial^{i+j+k}w_{t_1}}{\partial x_1{}^i\partial x_2{}^j\partial t^k}\right| \le C\mu^{-j},\ 1\le i+j+2k\le 2,$$
$$\left|\frac{\partial^{i+j+k}w_{t_1}}{\partial x_1{}^i\partial x_2{}^j\partial t^k}\right| \le C\mu^{-3}+C\varepsilon_1^{-1},\ i+j+2k=3,\ \left|\frac{\partial^{i+j+k}w_{t_2}}{\partial x_1{}^i\partial x_2{}^j\partial t^k}\right| \le C\mu^{-j},\ 1\le i+j+2k\le 3.$$

• *Finally, if $\Lambda\varepsilon_1 < \vartheta\mu^2 < \Lambda\varepsilon_2$ holds, we have*

$$|w_{l_1}| \le C\mathcal{G}_1^l(x_1),\ |w_{l_2}| \le C\mathcal{G}_2^l(x_1),\ \ |w_{b_1}| \le C\mathcal{G}_1^b(x_2),\ |w_{b_2}| \le C\mathcal{G}_2^b(x_2),$$
$$\left|\frac{\partial^{i+j+k} w_{l_1}}{\partial {x_1}^i \partial {x_2}^j \partial t^k}\right| \le C(\mu^i \varepsilon_1^{-i} \mathcal{G}_1^l(x_1) + \varepsilon_2^{-i/2}\mathcal{G}_2^l(x_1)),\ 1 \le i+j+2k \le 3,$$
$$\left|\frac{\partial^{i+j+k} w_{b_1}}{\partial {x_1}^i \partial {x_2}^j \partial t^k}\right| \le C(\mu^j \varepsilon_1^{-j} \mathcal{G}_1^b(x_2) + \varepsilon_2^{-j/2}\mathcal{G}_2^b(x_2)),\ 1 \le i+j+2k \le 3,$$
$$\left|\frac{\partial^{i+j+k} w_{l_2}}{\partial {x_1}^i \partial {x_2}^j \partial t^k}\right| \le C\varepsilon_2^{-i/2}\mathcal{G}_2^l(x_1),\ 1 \le i+j+2k \le 2,$$
$$\left|\frac{\partial^{i+j+k} w_{l_2}}{\partial {x_1}^i \partial {x_2}^j \partial t^k}\right| \le C\varepsilon_2^{-1}(\mu\varepsilon_1^{-1}\mathcal{G}_1^l(x_1) + \varepsilon_2^{-1/2}\mathcal{G}_2^l(x_1)),\ i+j+2k = 3,$$
$$\left|\frac{\partial^{i+j+k} w_{b_2}}{\partial {x_1}^i \partial {x_2}^j \partial t^k}\right| \le C\varepsilon_2^{-j/2}\mathcal{G}_2^b(x_2),\ 1 \le i+j+2k \le 2,$$
$$\left|\frac{\partial^{i+j+k} w_{b_2}}{\partial {x_1}^i \partial {x_2}^j \partial t^k}\right| \le C\varepsilon_2^{-1}(\mu\varepsilon_1^{-1}\mathcal{G}_1^b(x_2) + \varepsilon_2^{-1/2}\mathcal{G}_2^b(x_2)),\ i+j+2k = 3,$$
$$|w_{r_1}| \le C\mathcal{G}_1^r(x_1),\ |w_{r_2}| \le C\mathcal{G}_2^r(x_1),\ \ |w_{t_1}| \le C\mathcal{G}_1^t(x_2),\ |w_{t_2}| \le C\mathcal{G}_2^l(x_2),$$
$$\left|\frac{\partial^{i+j+k} w_{r_1}}{\partial {x_1}^i \partial {x_2}^j \partial t^k}\right| \le C(\mu^{-i} + \varepsilon_2^{-i/2}\mathcal{G}_2^r(x_1)),\ \left|\frac{\partial^{i+j+k} w_{t_1}}{\partial {x_1}^i \partial {x_2}^j \partial t^k}\right| \le C(\mu^{-j} + \varepsilon_2^{-j/2}\mathcal{G}_2^t(x_2)),\ 1 \le i+j+2k \le 3,$$
$$\left|\frac{\partial^{i+j+k} w_{r_2}}{\partial {x_1}^i \partial {x_2}^j \partial t^k}\right| \le C\varepsilon_2^{-i/2}\mathcal{G}_2^r(x_1),\ 1 \le i+j+2k \le 2,\ \left|\frac{\partial^{i+j+k} w_{r_2}}{\partial {x_1}^i \partial {x_2}^j \partial t^k}\right| \le C\varepsilon_2^{-1}(\mu^{-3} + \varepsilon_2^{-1/2}\mathcal{G}_2^r(x_1)),\ i+j+2k = 3,$$
$$\left|\frac{\partial^{i+j+k} w_{t_2}}{\partial {x_1}^i \partial {x_2}^j \partial t^k}\right| \le C\varepsilon_2^{-j/2}\mathcal{G}_2^t(x_2),\ 1 \le i+j+2k \le 2,\ \left|\frac{\partial^{i+j+k} w_{t_2}}{\partial {x_1}^i \partial {x_2}^j \partial t^k}\right| \le C\varepsilon_2^{-1}(\mu^{-3} + \varepsilon_2^{-1/2}\mathcal{G}_2^t(x_2)),\ i+j+2k = 3.$$

Theorem 2.6. *Let $\mathbf{s}_n$, $n = lb, br, rt, lt$, where $\mathbf{s}_n = (s_{n_1}, s_{n_2})^T$ satisfies problem (2.4). Then,*
• *If $\vartheta\mu^2 \le \Lambda\varepsilon_1$ holds, we have*

$$|\mathbf{s}_{k_1k_2}| \le C\mathcal{G}_2^{k_1}(x_1)\mathcal{G}_2^{k_2}(x_2),\ \ k_1 = l, r,\ k_2 = b, t,$$
$$\left|\frac{\partial^{i+j+k} s_{k_1k_{21}}}{\partial {x_1}^i \partial {x_2}^j \partial t^k}\right| \le C(\varepsilon_1^{(-i-j)/2}\mathcal{G}_1^{k_1}(x_1)\mathcal{G}_1^{k_2}(x_2) + \varepsilon_2^{(-i-j)/2}\mathcal{G}_2^{k_1}(x_1)\mathcal{G}_2^{k_2}(x_2)),\ \ 1 \le i+j+2k \le 3,\ k_1 = l, r,\ k_2 = b, t,$$

$$\left|\frac{\partial^{i+j+k} s_{k_1k_{22}}}{\partial {x_1}^i \partial {x_2}^j \partial t^k}\right| \le C\varepsilon_2^{(-i-j)/2}\mathcal{G}_2^{k_1}(x_1)\mathcal{G}_2^{k_2}(x_2),\ \ 1 \le i+j+2k \le 2,\ k_1 = l, r,\ k_2 = b, t,$$
$$\left|\frac{\partial^{i+j+k} s_{k_1k_{22}}}{\partial {x_1}^i \partial {x_2}^j \partial t^k}\right| \le C\varepsilon_2^{-2}(\varepsilon_1^{-1}\mathcal{G}_1^{k_1}(x_1)\mathcal{G}_1^{k_2}(x_2) + \varepsilon_2^{-1}\mathcal{G}_2^{k_1}(x_2)\mathcal{G}_2^{k_2}(x_2)),\ \ i+j+2k = 3,\ k_1 = l, r,\ k_2 = b, t.$$

• *If $\vartheta\mu^2 \ge \Lambda\varepsilon_2$ holds, we have*

$$|\mathbf{s}_{k_1k_2}| \le C\mathcal{G}_2^{k_1}(x_1)\mathcal{G}_2^{k_2}(x_2),\ \ k_1 = l, r,\ k_2 = b, t,$$
$$\left|\frac{\partial^{i+j+k} s_{lb_1}}{\partial {x_1}^i \partial {x_2}^j \partial t^k}\right| \le C\mu^{i+j}(\varepsilon_1^{-i-j}\mathcal{G}_1^l(x_1)\mathcal{G}_1^b(x_2) + \varepsilon_2^{-i-j}\mathcal{G}_2^l(x_1)\mathcal{G}_2^b(x_2)),\ \ 1 \le i+j+2k \le 3,$$

$$\left|\frac{\partial^{i+j+k}s_{lb_2}}{\partial x_1{}^i\partial x_2{}^j\partial t^k}\right| \le C\mu^{i+j+k}\varepsilon_2^{-i-j}\mathcal{G}_2^l(x_1)\mathcal{G}_2^b(x_2),\ 1\le i+j+2k\le 2,$$
$$\left|\frac{\partial^{i+j+k}s_{lb_2}}{\partial x_1{}^i\partial x_2{}^j\partial t^k}\right| \le C\mu^6\varepsilon_2^{-4}(\varepsilon_1^{-2}\mathcal{G}_1^l(x_1)\mathcal{G}_1^b(x_2)+\varepsilon_2^{-2}\mathcal{G}_2^l(x_1)\mathcal{G}_2^b(x_2)),\ i+j+2k=3,$$
$$\left|\frac{\partial^{i+j+k}s_{br_1}}{\partial x_1{}^i\partial x_2{}^j\partial t^k}\right| \le C\mu^{-i+j}(\varepsilon_1^{-j}\mathcal{G}_1^b(x_2)+\varepsilon_2^{-j}\mathcal{G}_2^b(x_2)),\ 1\le i+j+2k\le 3,$$
$$\left|\frac{\partial^{i+j+k}s_{br_2}}{\partial x_1{}^i\partial x_2{}^j\partial t^k}\right| \le C\mu^{-i+j}\varepsilon_2^{-j}\mathcal{G}_2^b(x_2),\ 1\le i+j+2k\le 3,\ \left|\frac{\partial^{i+j+k}s_{rt_1}}{\partial x_1{}^i\partial x_2{}^j\partial t^k}\right| \le C\mu^{-i-j},\ 1\le i+j+2k\le 2,$$
$$\left|\frac{\partial^{i+j+k}s_{rt_1}}{\partial x_1{}^i\partial x_2{}^j\partial t^k}\right| \le C(\mu^{-6}+\varepsilon_1^{-2}),\ i+j+2k=3,\ \left|\frac{\partial^{i+j+k}s_{rt_2}}{\partial x_1{}^i\partial x_2{}^j\partial t^k}\right| \le C\mu^{-i-j},\ 1\le i+j+2k\le 3,$$
$$\left|\frac{\partial^{i+j+k}s_{lt_1}}{\partial x_1{}^i\partial x_2{}^j\partial t^k}\right| \le C(\mu^{i-j}(\varepsilon_1^{-i}\mathcal{G}_1^l(x_1)+\varepsilon_2^{-i}\mathcal{G}_2^l(x_1))),\ 1\le i+j+2k\le 3,$$
$$\left|\frac{\partial^{i+j+k}s_{lt_2}}{\partial x_1{}^i\partial x_2{}^j\partial t^k}\right| \le C\mu^{i-j}\varepsilon_2^{-i}\mathcal{G}_2^l(x_1),\ 1\le i+j+2k\le 3.$$

• *Finally, if $\Lambda\varepsilon_1 < \vartheta\mu^2 < \Lambda\varepsilon_2$ holds, we have*

$$|\boldsymbol{s}_{lb_1}| \le C\mathcal{G}_1^l(x_1)\mathcal{G}_1^b(x_2),\ |\boldsymbol{s}_{lb_2}| \le C\mathcal{G}_2^l(x_1)\mathcal{G}_2^b(x_2),\ |\boldsymbol{s}_{br_1}| \le C\mathcal{G}_1^r(x_1)\mathcal{G}_1^b(x_2),$$
$$|\boldsymbol{s}_{br_2}| \le C\mathcal{G}_2^r(x_1)\mathcal{G}_2^b(x_2),\ |\boldsymbol{s}_{rt_1}| \le C\mathcal{G}_1^r(x_1)\mathcal{G}_1^t(x_2),\ |\boldsymbol{s}_{rt_2}| \le C\mathcal{G}_2^r(x_1)\mathcal{G}_2^t(x_2),$$
$$|\boldsymbol{s}_{lt_1}| \le C\mathcal{G}_1^l(x_1)\mathcal{G}_1^t(x_2),\ |\boldsymbol{s}_{lt_2}| \le C\mathcal{G}_2^l(x_1)\mathcal{G}_2^t(x_2),$$
$$\left|\frac{\partial^{i+j+k}s_{lb_1}}{\partial x_1{}^i\partial x_2{}^j\partial t^k}\right| \le C(\mu^{i+j}\varepsilon_1^{-i-j}\mathcal{G}_1^l(x_1)\mathcal{G}_1^b(x_2)+\varepsilon_2^{(-i-j)/2}\mathcal{G}_2^l(x_1)\mathcal{G}_2^b(x_2)),\ 1\le i+j+2k\le 3,$$
$$\left|\frac{\partial^{i+j+k}s_{lb_2}}{\partial x_1{}^i\partial x_2{}^j\partial t^k}\right| \le C\varepsilon_2^{(-i-j)/2}\mathcal{G}_2^l(x_1)\mathcal{G}_2^b(x_2),\ 1\le i+j+2k\le 2,$$
$$\left|\frac{\partial^{i+j+k}s_{lb_2}}{\partial x_1{}^i\partial x_2{}^j\partial t^k}\right| \le C\varepsilon_2^{-2}(\mu^2\varepsilon_1^{-2}\mathcal{G}_1^l(x_1)\mathcal{G}_1^b(x_2)+\varepsilon_2^{-1}\mathcal{G}_2^l(x_1)\mathcal{G}_2^b(x_2),\ i+j+2k=3,$$
$$\left|\frac{\partial^{i+j+k}s_{br_1}}{\partial x_1{}^i\partial x_2{}^j\partial t^k}\right| \le C(\mu^{-i+j}\varepsilon_1^{-j}\mathcal{G}_1^b(x_2)+\varepsilon_2^{(-1-j)/2}\mathcal{G}_2^r(x_1)\mathcal{G}_2^b(x_2),\ 1\le i+j+2k\le 3,$$
$$\left|\frac{\partial^{i+j+k}s_{br_2}}{\partial x_1{}^i\partial x_2{}^j\partial t^k}\right| \le C\varepsilon_2^{(-i-j)/2}\mathcal{G}_2^r(x_1)\mathcal{G}_2^b(x_2),\ 0\le i+j+2k\le 2,$$
$$\left|\frac{\partial^{i+j+k}s_{br_2}}{\partial x_1{}^i\partial x_2{}^j\partial t^k}\right| \le C\varepsilon_2^{-2}(\mu^{-2}\varepsilon_1^{-1}\mathcal{G}_1^b(x_2)+\varepsilon_2^{-1}\mathcal{G}_2^r(x_1)\mathcal{G}_2^b(x_2),\ i+j+2k=3,$$
$$\left|\frac{\partial^{i+j+k}s_{rt_1}}{\partial x_1{}^i\partial x_2{}^j\partial t^k}\right| \le C(\mu^{-i-j}+\varepsilon_2^{(-i-j)/2}\mathcal{G}_2^r(x_1)\mathcal{G}_2^t(x_2)),\ 1\le i+j+2k\le 3,$$
$$\left|\frac{\partial^{i+j+k}s_{rt_2}}{\partial x_1{}^i\partial x_2{}^j\partial t^k}\right| \le C\varepsilon_2^{(-i-j)/2}\mathcal{G}_2^r(x_1)\mathcal{G}_2^t(x_2),\ 1\le i+j+2k\le 2,$$

$$\left|\frac{\partial^{i+j+k}s_{rt_2}}{\partial x_1{}^i\partial x_2{}^j\partial t^k}\right| \le C\varepsilon_2^{-2}(\mu^{-6}+\varepsilon_2^{-1}\mathcal{G}_2^r(x_1)\mathcal{G}_2^t(x_2)),\ i+j+2k=3,$$
$$\left|\frac{\partial^{i+j+k}s_{lt_1}}{\partial x_1{}^i\partial x_2{}^j\partial t^k}\right| \le C(\mu^{i-j}\varepsilon_1^{-i}\mathcal{G}_1^l(x_1)+\varepsilon_2^{(-i-j)/2}\mathcal{G}_2^l(x_1)\mathcal{G}_2^t(x_2)),\ 1\le i+j+2k\le 3,$$

$$\left|\frac{\partial^{i+j+k} s_{lt_2}}{\partial x_1{}^i \partial x_2{}^j \partial t^k}\right| \leq C\varepsilon_2^{(-i-j)/2}\mathcal{G}_2^l(x_1)\mathcal{G}_2^t(x_2),\ 1 \leq i+j+2k \leq 2,$$
$$\left|\frac{\partial^{i+j+k} s_{lt_2}}{\partial x_1{}^i \partial x_2{}^j \partial t^k}\right| \leq C\varepsilon_2^{-2}(\mu^{-2}\varepsilon_1^{-1}\mathcal{G}_1^l(x_1) + \varepsilon_2^{-1}\mathcal{G}_2^l(x_1)\mathcal{G}_2^t(x_2)),\ i+j+2k = 3.$$

3. Discretization of the continuous problem

3.1. The spatial discretization

In this section, we propose a numerical scheme to solve problem (1.1). The approach begins by constructing a specially designed nonuniform mesh of the BS type tailored to the behavior of the exact solution. Once the mesh is defined, we formulate a finite difference method (FDM) over the domain $\overline{Q}^{N,M} = \{(x_{1i}, x_{2j}, t_n) : 0 \leq i, j \leq N,\ 0 \leq n \leq M\}$, where N and M denote the spatial and temporal discretization parameters, respectively.

The BS mesh

Following [21], the first step is the construction of the spatial mesh $\overline{\Omega}^N = \{x_{1i}, x_{2j}) : 0 \leq i, j \leq N\}$, where, for simplicity, the same number of grid points is considered in both the x_1 and x_2 directions. This mesh is formulated as the tensor product of appropriately designed 1D BS meshes, as depicted in Figures 1.

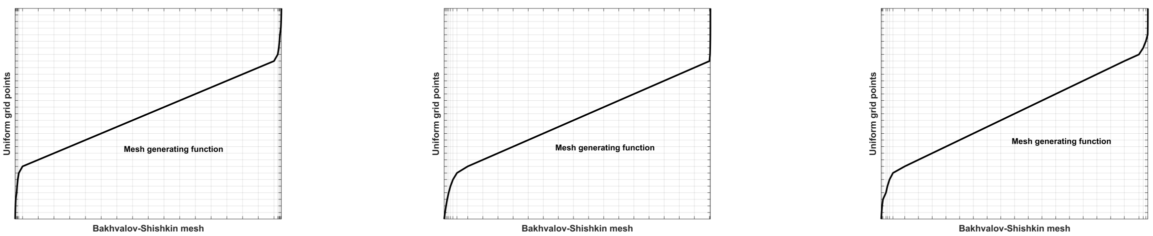

(a) BS mesh for Case 1; **(b)** BS mesh for Case 2; **(c)** BS mesh for Case 3.

Figure 1. BS mesh structures for Cases 1, 2, and 3.

We define the mesh points for the x_1-direction as $\{x_{1i}\}_{i=0}^N$, and analogously, the mesh points for the x_2-direction as $\{x_{2j}\}_{j=0}^N$. To do that, we distinguish several cases that depend on the value and the ratio between the diffusion and the convection parameters.

Case 1: If $\vartheta\mu^2 \leq \Lambda\varepsilon_1$, then we define the non uniform BS mesh by decomposing the unit interval $\overline{\Omega}_{x_1} := [0, 1]$ into five subintervals of the form

$$\overline{\Omega}_{x_1} := [0, 1] = [0, \tau_1] \cup [\tau_1, \tau_2] \cup [\tau_2, 1 - \tau_2] \cup [1 - \tau_2, 1 - \tau_1] \cup [1 - \tau_1, 1],$$

with the transition points τ_1, τ_2 defined by

$$\tau_1 = \min\left\{\frac{\tau_2}{2}, 2\sqrt{\frac{\varepsilon_1}{\Lambda\vartheta}}\ln N\right\},\ \tau_2 = \min\left\{\frac{1}{4}, 2\sqrt{\frac{\varepsilon_2}{\Lambda\vartheta}}\ln N\right\}. \tag{3.1a}$$

Each equal number of subintervals $[0,\tau_1],[\tau_1,\tau_2],[1-\tau_2,1-\tau_1],[1-\tau_1,1]$ are distributed by mesh-generating functions that are continuous, strictly increasing, and piecewise continuously differentiable, defined as follows:

$$\Phi(s)=\begin{cases}\Phi_l(s)=\begin{cases}-\ln\left(1-8(1-N^{-1})s\right), & s\in\left[0,\frac{1}{8}\right],\\ -\ln\left(1-8(1-N^{-1})(s-\frac{1}{8})\right), & s\in\left[\frac{1}{8},\frac{1}{4}\right],\end{cases} \Phi_r(s)=\begin{cases}\ln\left(1-8(1-N^{-1})(\frac{7}{8}-s)\right), & s\in\left[\frac{3}{4},\frac{7}{8}\right],\\ \ln\left(1-8(1-N^{-1})(1-s)\right), & s\in\left[\frac{7}{8},1\right].\end{cases}\end{cases}$$

In the remaining central subinterval $[\tau_2,1-\tau_2]$, the mesh is uniformly spaced with $N/2+1$ grid points. Then, the grid points along the x_1-direction are defined as

$$x_{1i}=\begin{cases}2\sqrt{\frac{\epsilon_1}{\Lambda\vartheta}}\Phi_l(s_i), & \text{if}\quad i=0,\dots,N/8,\\ \tau_1+2(\sqrt{\frac{\epsilon_2}{\Lambda\vartheta}}-\sqrt{\frac{\epsilon_1}{\Lambda\vartheta}})\Phi_l(s_i), & \text{if}\quad i=N/8+1,\dots,N/4,\\ \tau_2+\frac{2}{N}(1-2\tau_2)(i-\frac{N}{4}), & \text{if}\quad i=N/4+1,\dots,3N/4,\\ 1-\tau_1+2\left(\sqrt{\frac{\epsilon_2}{\Lambda\vartheta}}-\sqrt{\frac{\epsilon_1}{\Lambda\vartheta}}\right)\Phi_r(s_i), & \text{if}\quad i=3N/4+1,\dots,7N/8,\\ 1+2\sqrt{\frac{\epsilon_1}{\Lambda\vartheta}}\Phi_r(s_i), & \text{if}\quad i=7N/8+1,\dots,N,\end{cases}$$

where $s_i=\frac{i}{N}$.

Case 2: If $\vartheta\mu^2\geq\Lambda\varepsilon_2$, then we construct the non uniform BS mesh by decomposing the unit intervals $\overline{\Omega}_{x_1}$ into four subintervals of the form

$$\overline{\Omega}_{x_1}:=[0,1]=[0,\sigma]\cup[\sigma,1-\tau_2]\cup[1-\tau_2,1-\tau_1]\cup[1-\tau_1,1],$$

with the transition points τ_1,τ_2, and σ defined as

$$\tau_1=\min\left\{\frac{\tau_2}{2},\frac{2\varepsilon_1}{\mu\vartheta}\ln N\right\},\ \tau_2=\min\left\{\frac{1}{4},\frac{2\varepsilon_2}{\mu\vartheta}\ln N\right\},\ \sigma=\min\left\{\frac{1}{4},\frac{2\mu}{\Lambda}\ln N\right\}. \tag{3.2a}$$

The subintervals $[0,\sigma]$, $[1-\tau_2,1-\tau_1]$, and $[1-\tau_1,1]$ are each partitioned into an equal number of mesh intervals using piecewise continuously differentiable, monotonic mesh-generating functions $\Phi_l(s)$ and $\Phi_r(s)$, defined as follows:

$$\Phi(s)=\begin{cases}\Phi_l(s)=-\ln\left(1-4(1-N^{-1})s\right), \quad s\in\left[0,\frac{1}{4}\right],\\ \Phi_r(s)=\begin{cases}\ln\left(1-8(1-N^{-1})\left(\frac{7}{8}-s\right)\right), & s\in\left[\frac{3}{4},\frac{7}{8}\right],\\ \ln\left(1-8(1-N^{-1})(1-s)\right), & s\in\left[\frac{7}{8},1\right].\end{cases}\end{cases}$$

In the remaining central subinterval $[\sigma,1-\tau_2]$, the mesh is taken to be uniform, consisting of $N/2+1$ equally spatial grid points. Then, the grid points along the x_1-direction are defined as

$$x_{1i}=\begin{cases}2\frac{\mu}{\vartheta}\Phi_l(s_i), & \text{if}\quad i=0,\dots,N/4,\\ \sigma+\frac{2}{N}(1-\tau_2-\sigma)(i-\frac{N}{4}), & \text{if}\quad i=N/4+1,\dots,3N/4,\\ 1-\tau_1+(\frac{2\varepsilon_2}{\mu\vartheta}-\frac{2\varepsilon_1}{\mu\vartheta})\Phi_r(s_i), & \text{if}\quad i=3N/4+1,\dots,7N/8,\\ 1+\frac{2\varepsilon_1}{\mu\vartheta}\Phi_r(s_i), & \text{if}\quad i=7N/8+1,\dots,N,\end{cases}$$

where $s_i = \frac{i}{N}$.
Case 3: If $\Lambda\varepsilon_1 < \vartheta\mu^2 < \Lambda\varepsilon_2$, then we construct the non uniform BS mesh by decomposing the unit interval $\overline{\Omega}_{x_1} := [0, 1]$ into five subintervals of the form

$$\overline{\Omega}_{x_1} := [0,1] = [0,\sigma] \cup [\sigma,\tau_2] \cup [\tau_2, 1-\tau_2] \cup [1-\tau_2, 1-\tau_1] \cup [1-\tau_1, 1],$$

where the transition points $\tau_i,\ i = 1, 2$ and σ now are defined as

$$\tau_1 = \min\left\{\frac{\tau_2}{2}, \frac{2\varepsilon_1}{\mu\vartheta}\ln N\right\},\ \tau_2 = \min\left\{\frac{1}{4}, 2\sqrt{\frac{\varepsilon_2}{\Lambda\vartheta}}\ln N\right\},\ \sigma = \min\left\{\frac{\tau_2}{2}, \frac{2\mu}{\Lambda}\ln N\right\}. \tag{3.3a}$$

The subintervals $[0,\sigma]$, $[\sigma,\tau_2]$, $[1-\tau_2, 1-\tau_1]$, and $[1-\tau_1, 1]$ are each partitioned into an equal number of mesh intervals using the piecewise continuously differentiable functions $\Phi_l(s)$ and $\Phi_r(s)$, defined as follows:

$$\Phi(s) = \begin{cases} \Phi_l(s) = \begin{cases} -\ln\left(1 - 8(1-N^{-1})s\right), & s \in \left[0, \frac{1}{8}\right], \\ -\ln\left(1 - 8(1-N^{-1})(s - \frac{1}{8})\right), & s \in \left[\frac{1}{8}, \frac{1}{4}\right], \end{cases} \\ \Phi_r(s) = \begin{cases} \ln\left(1 - 8(1-N^{-1})\left(\frac{7}{8} - s\right)\right), & s \in \left[\frac{3}{4}, \frac{7}{8}\right], \\ \ln\left(1 - 8(1-N^{-1})(1-s)\right), & s \in \left[\frac{7}{8}, 1\right]. \end{cases} \end{cases}$$

In the remaining interior subinterval $[\tau_2, 1-\tau_2]$, a uniform mesh consisting of $N/2 + 1$ equally spaced grid points is employed. Then, the grid points along the x_1-axis are given by

$$x_{1i} = \begin{cases} 2\frac{\mu}{\vartheta}\Phi_l(s_i), & \text{if} \quad i = 0, \dots, N/8, \\ \sigma + 2(\sqrt{\frac{\varepsilon_2}{\Lambda\vartheta}} - \frac{\mu}{\vartheta})\Phi_l(s_i), & \text{if} \quad i = N/8+1, \dots, N/4, \\ \tau_2 + \frac{2}{N}(1-2\tau_2)(i - \frac{N}{4}), & \text{if} \quad i = N/4+1, \dots, 3N/4, \\ 1 - \tau_1 + 2(\sqrt{\frac{\varepsilon_2}{\Lambda\vartheta}} - \frac{\varepsilon_1}{\mu\vartheta})\Phi_r(s_i), & \text{if} \quad i = 3N/4+1, \dots, 7N/8, \\ 1 + 2\frac{\varepsilon_1}{\mu\vartheta}\Phi_r(s_i), & \text{if} \quad i = 7N/8+1, \dots, N, \end{cases}$$

where $s_i = \frac{i}{N}$. For each one of the cases, the step sizes are defined as $h_i = x_{1i} - x_{1i-1},\ i = 1, 2, ..., N,\ k_j = x_{2j} - x_{2j-1},\ j = 1, 2, ..., N,\ \bar{h}_i = h_i + h_{i+1},\ i = 1, 2, ..., N-1,\ \bar{k}_j = k_j + k_{j+1},\ j = 1, 2, ..., N-1$.
The boundaries of the spatial domain $\overline{\Omega}^N$ are denoted by

$$\Gamma_l^N = \left\{(0, x_{2j}) \,\middle|\, 0 \le j \le N\right\}, \Gamma_b^N = \left\{(x_{1i}, 0) \,\middle|\, 0 \le i \le N\right\},$$
$$\Gamma_r^N = \left\{(1, x_{2j}) \,\middle|\, 0 \le j \le N\right\}, \Gamma_t^N = \left\{(x_{1i}, 1) \,\middle|\, 0 \le i \le N\right\},$$

and $\Gamma^N = \Gamma_l^N \cup \Gamma_b^N \cup \Gamma_r^N \cup \Gamma_t^N$.

3.2. Time discretization and the FDM

The second step in constructing the fully discrete scheme is the time discretization. For this, the time interval $[0, T]$ is divided into M equal parts, giving the equidistant mes $\mathfrak{T}_t^M = \{t_n = n\Delta t, n = 0, ..., M, t_0 = 0, t_M = T, \Delta t = T/M\}$, where M is the number of time steps used in the discretization.

On an arbitrary mesh $\overline{Q}^{N,M}$, the discretization of (1.1) is carried out using the implicit Euler method in time combined with the classical upwind finite difference scheme in space, which is formulated as follows:

$$\begin{cases} \mathcal{L}^{N,N}_{\boldsymbol{\varepsilon},\boldsymbol{\mu}}\mathbf{Z} \equiv D_t^-\mathbf{Z} - \boldsymbol{\varepsilon}(\delta^2_{x_1x_1} + \delta^2_{x_2x_2})\mathbf{Z} + \boldsymbol{\mu}(\mathbf{A}_1(x_{1i}, x_{2j}, t_k)D^-_{x_1} + \mathbf{A}_2(x_{1i}, x_{2j}, t_k)D^-_{x_2})\mathbf{Z} \\ \qquad +\mathbf{B}(x_{1i}, x_{2j}, t_k)\vec{\mathbf{Z}} = \mathbf{f}(x_{1i}, x_{2j}, t_k),\ \forall (x_{1i}, x_{2j}, t_k) \in Q^{N,M}, \\ \mathbf{Z}(x_{1i}, x_{2j}, t_k) = \mathbf{q}(x_{1i}, x_{2j}, t_k),\ \forall (x_{1i}, x_{2j}, t_k) \in \partial\Omega^N \times \mathfrak{I}^M_t, \\ \mathbf{Z}(x_{1i}, x_{2j}, t_k) = \boldsymbol{\psi}(x_{1i}, x_{2j}, t_k),\ \forall (x_{1i}, x_{2j}, t_k) \in \Omega^N \times \{t_0\}, \\ \text{for}\, k = 1, ..., M. \end{cases} \tag{3.4}$$

As it is usual, the discrete differential operators $D^-_{x_1}$, $D^-_{x_2}$, D^-_t, $\delta^2_{x_1x_1}$, and $\delta^2_{x_2x_2}$ are defined by

$$D^+_{x_1}\mathbf{Z}(x_{1i}, x_{2j}, t_k) = \frac{\mathbf{Z}(x_{1i}, x_{2j}, t_k) - \mathbf{Z}(x_{1i}, x_{2j}, t_k)}{h_{i+1}},\ D^-_{x_1}\mathbf{Z}(x_{1i}, x_{2j}, t_k) = \frac{\mathbf{Z}(x_{1i}, x_{2j}, t_k) - \mathbf{Z}(x_{1i}, x_{2j}, t_k)}{h_i},$$

$$D^+_{x_2}\mathbf{Z}(x_{1i}, x_{2j}, t_k) = \frac{\mathbf{Z}(x_{1i}, x_{2j}, t_k) - \mathbf{Z}(x_{1i}, x_{2j}, t_k)}{k_{j+1}},\ D^-_{x_2}\mathbf{Z}(x_{1i}, x_{2j}, t_k) = \frac{\mathbf{Z}(x_{1i}, x_{2j}, t_k) - \mathbf{Z}(x_{1i}, x_{2j}, t_k)}{k_j},$$

$$D^-_t\mathbf{Z}(x_{1i}, x_{2j}, t_k) = \frac{\mathbf{Z}(x_{1i}, x_{2j}, t_k) - \mathbf{Z}(x_{1i}, x_{2j}, t_k)}{\Delta t},$$

$$\delta^2_{x_1x_1}\mathbf{Z}(x_{1i}, x_{2j}, t_k) = \frac{2}{\bar{h}_i}(D^+_{x_1}\mathbf{Z}(x_{1i}, x_{2j}, t_k) - D^-_{x_2}\mathbf{Z}(x_{1i}, x_{2j}, t_k)),$$

$$\delta^2_{x_2x_2}\mathbf{Z}(x_{1i}, x_{2j}, t_k) = \frac{2}{\bar{k}_j}(D^+_{x_2}\mathbf{Z}(x_{1i}, x_{2j}, t_k) - D^-_{x_2}\mathbf{Z}(x_{1i}, x_{2j}, t_k)),$$

for $i, j = 1, 2, \ldots, N-1$.

Assumption 1. *We assume that for the case $\vartheta\mu^2 \geq \Lambda\varepsilon_2$, it holds that $\varepsilon_2/\mu < N^{-1}$ and $\mu < N^{-1}$. For the case $\vartheta\mu^2 \leq \Lambda\varepsilon_1$, it holds that $\sqrt{\varepsilon_2} < N^{-1}$, and for the case $\Lambda\varepsilon_1 < \vartheta\mu^2 < \Lambda\varepsilon_2$, it holds that $\varepsilon_1/\mu < N^{-1}, \mu < N^{-1}$, and $\sqrt{\varepsilon_2} < N^{-1}$ as generally is the case in practice.*

Assumption 2. *The mesh-generating functions are assumed to be piecewise differentiable and to satisfy*

$$\max_{s\in[0,1/4]} \Phi_l{}'(s) \leq CN \text{ and } \max_{s\in[3/4,1]} \Phi_r{}'(s) \leq CN,$$

or equivalently,

$$\max_{s\in[0,1/4]} \frac{|\Phi_l{}'|}{\Phi_l} \leq CN \text{ and } \max_{s\in[3/4,1]} \frac{|\Phi_r{}'|}{\Phi_r} \leq CN.$$

Assumption 3. *Finally, we also assume that it holds*

$$\int_0^{1/4} \{\Phi_l'(s)\}^2 ds \leq CN \text{ and } \int_{3/4}^1 \{\Phi_r'(s)\}^2 ds \leq CN.$$

Using Assumption 2, it follows that $h_i \leq CN^{-1}, k_j \leq CN^{-1}$ for $1 \leq i, j \leq N$.

Analogous to the continuous problem, a discrete maximum principle can be established for the discrete operator $\mathcal{L}^{N,N}_{\boldsymbol{\varepsilon},\boldsymbol{\mu}}$.

Lemma 3.1 (Discrete maximum principle). *Let $\mathcal{L}_{\varepsilon,\vec{\mu}}^{N,N}$ be the discrete operator given in (3.4). If $\boldsymbol{v}(x_{1i}, x_{2j}, t_k) \geq \mathbf{0}$ on $\Gamma^N \times \mathfrak{I}_t^M \cup \Omega^N \times \{0\}$ and $\mathcal{L}_{\varepsilon,\mu}^{N,N}\boldsymbol{v}(x_{1i}, x_{2j}, t_k) \geq \mathbf{0}$, $\forall(x_{1i}, x_{2j}, t_k) \in Q^{N,M}$, then $\boldsymbol{v}(x_{1i}, x_{2j}, t_k) \geq \mathbf{0}$, $\forall(x_{1i}, x_{2j}, t_k) \in \overline{Q}^{N,M}$.*

Proof. This lemma can be proved by following the ideas presented in [7, 10]. □

Lemma 3.2 (Discrete stability result). *Let $\boldsymbol{v}(x_{1i}, x_{2j}, t_k)$ be the solution of (3.4). Then, it holds that*

$$\|\boldsymbol{v}(x_{1i}, x_{2j}, t_k)\|_{\overline{Q}^{N,M}} \leq \frac{1}{\vartheta}\|\mathcal{L}_{\varepsilon,\mu}^{N,N}\boldsymbol{v}\|_{Q^{N,M}} + \max\left\{\|\boldsymbol{v}\|_{\partial\Omega^N\times\mathfrak{I}_t^M}, \|\boldsymbol{v}\|_{\Omega^N\times\{0\}}\right\}.$$

Proof. This result follows directly from Lemma 3.1. □

4. Uniform convergence of the fully discrete scheme

This section gives a rigorous error analysis of the proposed numerical scheme and establishes its uniform convergence. To do that, first we decompose the numerical solution into its regular, layer, and corner components, following an approach analogous to that employed for the corresponding continuous solution; then, we have $\mathbf{Z}(x_{1i}, x_{2j}, t_k) = \mathbf{R}(x_{1i}, x_{2j}, t_k) + \mathbf{W}(x_{1i}, x_{2j}, t_k) + \mathbf{S}(x_{1i}, x_{2j}, t_k)$, where

$$\mathbf{W}(x_{1i}, x_{2j}, t_k) = \mathbf{W}_l(x_{1i}, x_{2j}, t_k) + \mathbf{W}_r(x_{1i}, x_{2j}, t_k) + \mathbf{W}_b(x_{1i}, x_{2j}, t_k) + \mathbf{W}_t(x_{1i}, x_{2j}, t_k),$$
$$\mathbf{S}(x_{1i}, x_{2j}, t_k) = \mathbf{S}_{lb}(x_{1i}, x_{2j}, t_k) + \mathbf{S}_{br}(x_{1i}, x_{2j}, t_k) + \mathbf{S}_{rt}(x_{1i}, x_{2j}, t_k) + \mathbf{S}_{lt}(x_{1i}, x_{2j}, t_k).$$

Furthermore, the regular component $\mathbf{R}(x_{1i}, x_{2j}, t_k)$ is defined as the solution of the associated problem

$$\begin{cases} \mathcal{L}_{\varepsilon,\mu}^{N,N}\mathbf{R}(x_{1i}, x_{2j}, t_k) = \mathbf{f}(x_{1i}, x_{2j}, t_k), & \forall(x_{1i}, x_{2j}, t_k) \in Q^{N,M}, \\ \mathbf{R}(x_{1i}, x_{2j}, t_k) = \mathbf{r}(x_{1i}, x_{2j}, t_k), & \forall(x_{1i}, x_{2j}, t_k) \in \partial Q^{N,M}. \end{cases} \tag{4.1}$$

Similarly, the layer component $\mathbf{W}(x_{1i}, x_{2j}, t_k)$ and the corner component $\mathbf{S}(x_{1i}, x_{2j}, t_k)$ are introduced as the solutions of the following numerical problems:

$$\begin{cases} \mathcal{L}_{\varepsilon,\mu}^{N,N}\mathbf{W}(x_{1i}, x_{2j}, t_k) = \mathbf{0}, & \forall(x_{1i}, x_{2j}, t_k) \in Q^{N,M}, \\ \mathbf{W}(x_{1i}, x_{2j}, t_k) = \mathbf{w}(x_{1i}, x_{2j}, t_k), & \forall(x_{1i}, x_{2j}, t_k) \in \partial Q^{N,M}, \end{cases} \tag{4.2}$$

for the layer component, and

$$\begin{cases} \mathcal{L}_{\varepsilon,\mu}^{N,N}\mathbf{S}(x_{1i}, x_{2j}, t_k) = \mathbf{0}, & \forall(x_{1i}, x_{2j}, t_k) \in Q^{N,M}, \\ \mathbf{S}(x_{1i}, x_{2j}, t_k) = \mathbf{s}(x_{1i}, x_{2j}, t_k), & \forall(x_{1i}, x_{2j}, t_k) \in \partial Q^{N,M}, \end{cases} \tag{4.3}$$

for the corner component, respectively.

To bound the error estimates corresponding to the boundary and corner layer components, we utilize an argument that relies on appropriately constructed barrier functions; these functions are defined by

$$\begin{cases} \mathcal{B}_1^{l,N}(x_{1i}) = \prod_{\iota=1}^{i}\left(1 + \dfrac{\vartheta\mu h_\iota}{2\varepsilon_1}\right)^{-1}, & \mathcal{B}_2^{l,N}(x_{1i}) = \prod_{\iota=1}^{i}\left(1 + \dfrac{\vartheta\mu h_\iota}{2\varepsilon_2}\right)^{-1}, & \vartheta\mu^2 \leq \Lambda\varepsilon_1, \\ \mathcal{B}_1^{l,N}(x_{1i}) = \prod_{\iota=1}^{i}\left(1 + \dfrac{\vartheta\mu h_\iota}{2\varepsilon_1}\right)^{-1}, & \mathcal{B}_2^{l,N}(x_{1i}) = \prod_{\iota=1}^{i}\left(1 + \dfrac{\vartheta\mu h_\iota}{2\varepsilon_2}\right)^{-1}, & \vartheta\mu^2 \geq \Lambda\varepsilon_2, \\ \mathcal{B}_1^{l,N}(x_{1i}) = \prod_{\iota=1}^{i}\left(1 + \left(\dfrac{\vartheta\mu}{2\varepsilon_1}\right)h_\iota\right)^{-1}, & \mathcal{B}_2^{l,N}(x_{1i}) = \prod_{\iota=1}^{i}\left(1 + \sqrt{\left(\dfrac{\Lambda\vartheta}{\varepsilon_2}\right)}h_\iota\right)^{-1}, & \Lambda\varepsilon_1 < \vartheta\mu^2 < \Lambda\varepsilon_2, \end{cases}$$

with $\mathcal{B}_1^{l,N}(x_{10}) = \mathcal{B}_2^{l,N}(x_{10}) = 1$.

Lemma 4.1. *Let $\mathbf{r}(x_1, x_2, t)$ denote the solution of (2.2) and $\mathbf{R}(x_{1i}, x_{2j}, t_k)$ represent the corresponding discrete solution of (4.1). Then, for each of the following cases, $\vartheta\mu^2 \le \Lambda\varepsilon_1$, $\vartheta\mu^2 \ge \Lambda\varepsilon_2$, and $\Lambda\varepsilon_1 < \vartheta\mu^2 < \Lambda\varepsilon_2$, it holds that*

$$|\boldsymbol{R}(x_{1i}, x_{2j}, t_k) - \boldsymbol{r}(x_{1i}, x_{2j}, t_k)| \le C(N^{-1} + \Delta t).$$

Proof. By applying Taylor series, it can be readily shown that the truncation error corresponding to the smooth component (4.1) satisfies

$$\begin{aligned}|\mathcal{L}^{N,N}_{\varepsilon,\mu}(\mathbf{R} - \mathbf{r})(x_{1i}, x_{2j}, t_k)| \le C\Big[\Delta t\Big\|\frac{\partial^2\mathbf{r}}{\partial t^2}\Big\| + (h_i + h_{i+1})\Big(\boldsymbol{\varepsilon}\Big\|\frac{\partial^3\mathbf{r}}{\partial {x_1}^3}\Big\| + \boldsymbol{\mu}\Big\|\frac{\partial^2\mathbf{r}}{\partial {x_1}^2}\Big\|\Big) \\ + (k_j + k_{j+1})\Big(\boldsymbol{\varepsilon}\Big\|\frac{\partial^3\mathbf{r}}{\partial {x_2}^3}\Big\| + \boldsymbol{\mu}\Big\|\frac{\partial^2\mathbf{r}}{\partial {x_2}^2}\Big\|\Big)\Big]. \end{aligned} \tag{4.4}$$

Now, using the Assumptions 1, 2, and 3 and the derivative bounds of $\mathbf{r}$ provided in Theorem (2.4), it follows that

$$|\mathcal{L}^{N,N}_{\varepsilon,\mu}(\mathbf{R} - \mathbf{r})(x_{1i}, x_{2j}, t_k)| \le \begin{cases} \begin{pmatrix} CN^{-1}(\sqrt{\varepsilon_1} + \mu) + C\Delta t \\ CN^{-1}(\varepsilon_2 + \mu) + C\Delta t \end{pmatrix}, & \text{if } \vartheta\mu^2 \le \Lambda\varepsilon_1, \\ \begin{pmatrix} CN^{-1}(1 + \mu) + C\Delta t \\ CN^{-1}(\varepsilon_2 + \mu) + C\Delta t \end{pmatrix}, & \text{if } \vartheta\mu^2 \ge \Lambda\varepsilon_2, \\ \begin{pmatrix} CN^{-1}(1 + \mu) + C\Delta t \\ CN^{-1}(\sqrt{\varepsilon_2}) + C\Delta t \end{pmatrix}, & \text{if } \Lambda\varepsilon_1 < \vartheta\mu^2 < \Lambda\varepsilon_2. \end{cases}$$

By applying Lemma 3.1 to $C(N^{-1} + \Delta t) \pm (\mathbf{R} - \mathbf{r})(x_{1i}, x_{2j}, t_k)$ over the domain Ω^N, it follows directly that, for all considered cases, it holds that

$$|(\mathbf{R} - \mathbf{r})(x_{1i}, x_{2j}, t_k)| \le C(N^{-1} + \Delta t), \tag{4.5}$$

which is the required result. □

Lemma 4.2. *Let $\boldsymbol{w}_n$ and $\boldsymbol{W}_n$ denote the exact and discrete solutions of* (2.3) *and* (4.2)*, respectively. For $\vartheta\mu^2 \le \Lambda\varepsilon_1$, the error of the boundary layer functions satisfies*

$$|\boldsymbol{W}_n(x_{1i}, x_{2j}, t_k) - \boldsymbol{w}_n(x_{1i}, x_{2j}, t_k)| \le C(N^{-1} + \Delta t), \ \ n = l, b, r, t.$$

Proof. From the Theorem (2.5), it follows that

$$|\mathbf{w}_l(x_{1i}, x_{2j}, t_k)| \le C\mathcal{G}^l_2(x_{1i}).$$

So, for all $(x_{1i}, x_{2j}, t_k) \in [\tau_2, 1) \times (0, 1) \times (0, T]$, we have

$$|\boldsymbol{w}_l(x_{1i}, x_{2j}, t_k)| \le C\mathcal{G}^l_2(x_{1i}) \le C\mathcal{G}^l_2(x_{1N/4}) = Ce^{-2\log N} = CN^{-2}. \tag{4.6}$$

Also, it is straightforward to see that

$$|\boldsymbol{W}_l(x_{1i}, x_{2j}, t_k)| \le C\mathcal{B}^{l,N}_1(x_{1i}) \le C\mathcal{B}^{l,N}_1(x_{1N/4}), \quad \forall i \ge N/4, 1 \le j \le N, 1 \le k \le M.$$

Using the methodology given in ([17], Section 4.2), we can obtain

$$|\boldsymbol{W}_l(x_{1i}, x_{2j}, t_k)| \le CN^{-1}, \quad \forall\ i \ge N/4, 1 \le j \le N, 1 \le k \le M.$$

Hence, for all $(x_{1i}, x_{2j}, t_k) \in [\tau_2, 1) \times (0, 1) \times (0, T]$, from (4.6) and the above equation, we have

$$|(\boldsymbol{W}_l - \boldsymbol{w}_l)(x_{1i}, x_{2j}, t_k)| \le |\boldsymbol{W}_l| + |\boldsymbol{w}_l| \le CN^{-1}. \tag{4.7}$$

To obtain suitable error bounds in the regions $0 < x_{1i} < \tau_1$, $\tau_1 < x_{1i} < \tau_2$, by using (4.2), Theorem 2.5, $(h_i + h_{i+1}) \le N^{-1}$, and $(k_j + k_{j+1}) \le N^{-1}$, we have

$$\begin{aligned}\|\boldsymbol{\mathcal{L}}^{N,N}_{\boldsymbol{\varepsilon},\boldsymbol{\mu}}(\mathbf{W}_l - \mathbf{w}_l)\| &\le C\Big[\Delta t\Big\|\frac{\partial^2 \mathbf{w}_l}{\partial t^2}\Big\| + (h_i + h_{i+1})\Big(\boldsymbol{\varepsilon}\Big\|\frac{\partial^3 \mathbf{w}_l}{\partial {x_1}^3}\Big\| + \boldsymbol{\mu}\Big\|\frac{\partial^2 \mathbf{w}_l}{\partial {x_1}^2}\Big\|\Big) + (k_j + k_{j+1})\Big(\boldsymbol{\varepsilon}\Big\|\frac{\partial^3 \mathbf{w}_l}{\partial {x_2}^3}\Big\| + \boldsymbol{\mu}\Big\|\frac{\partial^2 \vec{\mathbf{w}}_l}{\partial {x_2}^2}\Big\|\Big)\Big] \\ &\le C\begin{pmatrix} N^{-1}(\varepsilon_1^{-1/2}\mathcal{G}^l_1(x_{1i-1}) + \varepsilon_2^{-1/2}\mathcal{G}^l_2(x_{1i-1})) + \Delta t \\ N^{-1}(\varepsilon_1^{-1/2}\mathcal{G}^l_1(x_{1i-1}) + \varepsilon_2^{-1/2}\mathcal{G}^l_2(x_{1i-1})) + \Delta t \end{pmatrix}.\end{aligned}$$

Choosing now the barrier function for the $\boldsymbol{w}_l$ as

$$\Phi^{\pm}(x_{1i}, x_{2j}, t_k) = \begin{pmatrix} C[\frac{N^{-1}}{\sqrt{\varepsilon_1}\ln N}(\tau_2 - x_{1i}) + \Delta t] \pm (W_{l_1} - w_{l_1})(x_{1i}, x_{2j}, t_k) \\ C[\frac{N^{-1}}{\sqrt{\varepsilon_2}\ln N}(\tau_2 - x_{1i}) + \Delta t] \pm (W_{l_2} - w_{l_2})(x_{1i}, x_{2j}, t_k) \end{pmatrix},$$

by Lemma 3.1, we obtain the bound

$$\begin{aligned}|(\boldsymbol{W}_l - \boldsymbol{w}_l)(x_{1i}, x_{2j}, t_k)| \le & C\begin{pmatrix} [\frac{N^{-1}}{\sqrt{\varepsilon_1}\ln N}(\tau_2 - x_{1i}) + \Delta t] \\ [\frac{N^{-1}}{\sqrt{\varepsilon_2}\ln N}(\tau_2 - x_{1i}) + \Delta t] \end{pmatrix} \\ \le & C\begin{pmatrix} [\frac{N^{-1}\tau_2}{\sqrt{\varepsilon_1}\ln N} + \Delta t] \\ [\frac{N^{-1}\tau_2}{\sqrt{\varepsilon_2}\ln N} + \Delta t] \end{pmatrix},\end{aligned}$$

and therefore

$$|(\boldsymbol{W}_l - \boldsymbol{w}_l)(x_{1i}, x_{2j}, t_k)| \le C(N^{-1} + \Delta t).$$

Similarly, error bounds can also be shown for the other layer components $\mathbf{w}_r$, , $\mathbf{w}_b$, and $\mathbf{w}_t$ when $\vartheta\mu^2 \le \Lambda\varepsilon_1$. □

Lemma 4.3. *Let $\boldsymbol{w}_n$ and $\boldsymbol{W}_n$ be the exact and discrete solutions of* (2.3) *and* (4.2)*, respectively. For $\vartheta\mu^2 \ge \Lambda\varepsilon_2$, it holds that*

$$|\boldsymbol{W}_n(x_{1i}, x_{2j}, t_k) - \boldsymbol{w}_n(x_{1i}, x_{2j}, t_k)| \le C(N^{-1} + \Delta t),\ \ n = l, b, r, t.$$

Proof. The proof is provided in A. □

In the same way, similar bounds can be established for the errors associated with the other layer components $\mathbf{w}_r$, $\mathbf{w}_b$, and $\mathbf{w}_t$, corresponding to the case $\vartheta\mu^2 > \Lambda\varepsilon_2$.

Lemma 4.4. *For $\Lambda\varepsilon_1 < \vartheta\mu^2 < \Lambda\varepsilon_2$, the exact solution $\boldsymbol{w}_n$ of* (2.3) *and its discrete component $\boldsymbol{W}_n$ of* (4.2) *satisfy the following estimate:*

$$|\boldsymbol{W}_n(x_{1i}, x_{2j}, t_k) - \boldsymbol{w}_n(x_{1i}, x_{2j}, t_k)| \leq C(N^{-1} + \Delta t), \ \ n = l, b, r, t.$$

Proof. The proof is given in B. □

The final step is devoted to the error analysis of the corner components. As before, we focus on the corner component $\mathbf{s}_{lb}$, while similar arguments can be applied to the remaining corner components. Once again, it is necessary to consider the following three distinct cases $\vartheta\mu^2 \leq \Lambda\varepsilon_1$, $\vartheta\mu^2 \geq \Lambda\varepsilon_2$, and $\Lambda\varepsilon_1 < \vartheta\mu^2 < \Lambda\varepsilon_2$.

Lemma 4.5. *For $n = lb, br, rt, lt$, let $\mathbf{s}_n$ and $\mathbf{S}_n$ denote the exact and numerical solutions of* (2.4) *and* (4.3)*, respectively. Then, for $\vartheta\mu^2 \geq \Lambda\varepsilon_2$, the following estimate holds:*

$$|\boldsymbol{S}_n(x_{1i}, x_{2j}, t_k) - \boldsymbol{s}_n(x_{1i}, x_{2j}, t_k)| \leq C(N^{-1} + \Delta t).$$

Proof. According to the results established in Theorem 2.6, the truncation error associated with the corner component $\mathbf{s}_{lb}$ satisfies

$$\begin{aligned} \|\boldsymbol{\mathcal{L}}^{N,N}_{\boldsymbol{\varepsilon},\boldsymbol{\mu}}(\mathbf{S}_{lb} - \mathbf{s}_{lb})\| \leq C\Big[\Delta t\Big\|\frac{\partial^2 \mathbf{s}_{lb}}{\partial t^2}\Big\| + (h_i + h_{i+1})\Big(\boldsymbol{\varepsilon}\Big\|\frac{\partial^3 \vec{\mathbf{s}}_{lb}}{\partial {x_1}^3}\Big\| + \boldsymbol{\mu}\Big\|\frac{\partial^2 \vec{\mathbf{s}}_{lb}}{\partial {x_1}^2}\Big\|\Big) \\ + (k_j + k_{j+1})\Big(\boldsymbol{\varepsilon}\Big\|\frac{\partial^3 \mathbf{s}_{lb}}{\partial {x_2}^3}\Big\| + \boldsymbol{\mu}\Big\|\frac{\partial^2 \mathbf{s}_{lb}}{\partial {x_2}^2}\Big\|\Big)\Big]. \end{aligned} \tag{4.8}$$

If $\tau_1 = 1/8$, $\tau_2 = 1/4$, and $\sigma_1 = 1/4$, the proof can be obtained directly by applying standard techniques on uniform meshes, using that $\mu^{-1}\varepsilon_1 \leq CN^{-1}$, $\mu^{-1}\varepsilon_2 \leq CN^{-1}$, and $\mu \leq CN^{-1}$. Then, by applying Theorem 2.6 to (4.8), we obtain

$$|\boldsymbol{\mathcal{L}}^{N,N}_{\boldsymbol{\varepsilon},\boldsymbol{\mu}}(\boldsymbol{S}_{lb} - \boldsymbol{s}_{lb})| \leq C\begin{pmatrix} \mu^3\varepsilon_1^{-2}(\mathcal{B}_1^l(x_{1i-1})\mathcal{B}_1^b(x_{2j-1})) + \mu^3\varepsilon_2^{-2}(\mathcal{B}_2^l(x_{1i-1})\mathcal{B}_2^b(x_{2j-1})) + \Delta t \\ \mu^3\varepsilon_1^{-1}\varepsilon_2^{-1}(\mathcal{B}_1^l(x_{1i-1})\mathcal{B}_1^b(x_{2j-1})) + \mu^3\varepsilon_2^{-2}(\mathcal{B}_2^l(x_{1i-1})\mathcal{B}_2^b(x_{2j-1})) + \Delta t \end{pmatrix}. \tag{4.9}$$

Now, considering the barrier function from Lemma 4.3 (see (A.3)) in $\overline{\Omega}^N$ and applying Lemma 3.1, we deduce that

$$|(\mathbf{S}_{lb} - \mathbf{s}_{lb})(x_{1i}, x_{2j}, t_k)| \leq C\begin{pmatrix} \mu + \Delta t \\ \mu + \Delta t \end{pmatrix} \leq C(N^{-1} + \Delta t).$$

Next, from (4.3), for the case $\tau_2 = \dfrac{\varepsilon_2}{\mu\vartheta}\ln N$, considering the mesh points (x_{1i}, x_{2j}, t_k) with $(0 < i, j < N) \setminus (0 < i, j < N/4), 0 \leq k \leq M$, we obtain

$$\begin{aligned} |(S_{lb_1} - s_{lb_1})(x_{1i}, x_{2j}, t_k)| &\leq |S_{lb_1}(x_{1i}, x_{2j}, t_k)| + |s_{lb_1}(x_{1i}, x_{2j}, t_k)| \leq C\min(\mathcal{B}_2^{l,N}(x_{1i}), \mathcal{B}_2^{b,N}(x_{2j})) \\ &\leq C\min(\mathcal{B}_2^{l,N}(\tau_2), \mathcal{B}_2^{b,N}(\tau_2)) \leq CN^{-1}. \end{aligned} \tag{4.10}$$

Similarly, we can deduce that it holds

$$|(S_{lb_2} - s_{lb_2})(x_{1i}, x_{2j}, t_k)| \leq CN^{-1}. \tag{4.11}$$

When $\tau_2 = \dfrac{\varepsilon_2}{\mu\vartheta}\ln N$, there are two different cases: $2\varepsilon_1 \geq \varepsilon_2$ and $2\varepsilon_1 < \varepsilon_2$, respectively. In the case $\dfrac{\varepsilon_2}{2} \leq \varepsilon_1 \leq \varepsilon_2$, for $N/8 \leq i \leq N/4$, $0 \leq j \leq N/4$, $0 \leq k \leq M$, $\tau_2 \leq \dfrac{2\varepsilon_1}{\mu\vartheta}\ln N$. Hence, we obtain

$$|\mathcal{L}^{N,N}_{\varepsilon,\mu}(\mathbf{S}_{lb}-\mathbf{s}_{lb})(x_{1i},x_{2j},t_k)| \leq C\begin{pmatrix}\varepsilon_1^{-1}\mu^2(\mathcal{B}_1^l(x_{1i-1})\mathcal{B}_1^b(x_{2j-1})) + \varepsilon_2^{-1}\mu^2(\mathcal{B}_2^l(x_{1i-1})\mathcal{B}_2^b(x_{2j-1})) + \Delta t\\ \varepsilon_2^{-1}\mu^2(\mathcal{B}_2^l(x_{1i-1})\mathcal{B}_2^b(x_{2j-1})) + \Delta t\end{pmatrix}.$$

In the case $\varepsilon_2 > 2\varepsilon_1$, for $N/8 \leq i \leq N/4$, $0 \leq j \leq N/4$, $0 \leq k \leq M$, we have

$$|\mathcal{L}^{N,N}_{\varepsilon,\mu}(\mathbf{S}_{lb}-\mathbf{s}_{lb})(x_{1i},x_{2j},t_k)| \leq \begin{pmatrix}C\varepsilon_1^{-1}\mu^2(\mathcal{B}_1^l(x_{1i-1})\mathcal{B}_1^b(x_{2j-1})) + C\varepsilon_2^{-1}\mu^2(\mathcal{B}_2^l(x_{1i-1})\mathcal{B}_2^b(x_{2j-1})) + C\Delta t\\ C\varepsilon_2^{-1}\mu^2(\mathcal{B}_1^l(x_{1i-1})\mathcal{B}_1^b(x_{2j-1})) + C\varepsilon_2^{-1}\mu^2(\mathcal{B}_2^l(x_{1i-1})\mathcal{B}_2^b(x_{2j-1})) + C\Delta t\end{pmatrix}.$$

For $0 \leq i \leq N/8$, $0 \leq j \leq N/4$, $0 \leq k \leq M$, $\tau_1 \leq \dfrac{\varepsilon_1}{\vartheta}\ln N$, it follows that the local error satisfies

$$|\mathcal{L}^{N,N}_{\varepsilon,\mu}(\mathbf{S}_{lb}-\mathbf{s}_{lb})(x_{1i},x_{2j},t_k)| \leq C\begin{pmatrix}\varepsilon_1^{-1}\mu^2(\mathcal{B}_1^l(x_{1i-1})\mathcal{B}_1^b(x_{2j-1})) + \varepsilon_2^{-1}\mu^2(\mathcal{B}_2^l(x_{1i-1})\mathcal{B}_2^b(x_{2j-1})) + \Delta t\\ \varepsilon_2^{-1}\mu^2(\mathcal{B}_2^l(x_{1i-1})\mathcal{B}_2^b(x_{2j-1})) + \Delta t\end{pmatrix}.$$

For $0 \leq i \leq \frac{N}{4}$, $0 \leq j \leq \frac{N}{4}$, and $0 \leq k \leq M$, by employing the barrier functions $\boldsymbol{\psi}(x_{1i})$ and $\boldsymbol{\psi}(x_{2j})$ defined in Lemma 4.3 (see (A.7)), we obtain

$$|(\mathbf{S}_{lb}-\mathbf{s}_{lb})(x_{1i},x_{2j},t_k)| \leq CN^{-1} + C\Delta t,\ \ 0 \leq i \leq N/4,\ 0 \leq j \leq N/4,\ 0 \leq k \leq M. \tag{4.12}$$

From (4.10), (4.11), and (4.12), for $\tau_2 = \dfrac{\varepsilon_2}{\mu\vartheta}\ln N$, it follows that

$$|(\mathbf{S}_{lb}-\mathbf{s}_{lb})(x_{1i},x_{2j},t_k)| \leq CN^{-1} + C\Delta t.$$

Next, we consider the case where $\tau_2 = 1/4$, $\sigma_1 = 1/4$, and $\tau_1 = \dfrac{\varepsilon_1}{\mu\vartheta}\ln N$. Under these assumptions, it holds that $\mu\varepsilon_2^{-1} \leq CN^{-1}$. For $(x_{1i},x_{2j},t_k) \in (0,\tau_1]\times(0,\tau_2]\times(0,T]$, the mesh sizes satisfy $h_i,\ k_j \leq \dfrac{\varepsilon_1}{\mu}$.

Therefore, using the truncation error bound from (4.8), we deduce

$$|\mathcal{L}^{N,N}_{\varepsilon,\mu}(\mathbf{S}_{lb}-\mathbf{s}_{lb})(x_{1i},x_{2j},t_k)| \leq C\begin{pmatrix}\varepsilon_1^{-1}\mu^2(\mathcal{B}_1^l(x_{1i-1})\mathcal{B}_1^b(x_{2j-1})) + \varepsilon_2^{-1}\mu^2(\mathcal{B}_2^l(x_{1i-1})\mathcal{B}_2^b(x_{2j-1})) + \Delta t\\ \varepsilon_2^{-1}\mu^2(\mathcal{B}_2^l(x_{1i-1})\mathcal{B}_2^b(x_{2j-1})) + \Delta t\end{pmatrix}.$$

For $(x_{1i},x_{2j},t_k) \in [\tau_1,\tau_2]\times(0,\tau_2]\times(0,T]$, applying (4.8) with Lemma 2.6, it follows that

$$|\mathcal{L}^{N,N}_{\varepsilon,\mu}(\mathbf{S}_{lb}-\mathbf{s}_{lb})(x_{1i},x_{2j},t_k)| \leq \begin{pmatrix}C\varepsilon_1^{-1}\mu^2(\mathcal{B}_1^l(x_{1i-1})\mathcal{B}_1^b(x_{2j-1})) + C\varepsilon_2^{-1}\mu^2(\mathcal{B}_2^l(x_{1i-1})\mathcal{B}_2^b(x_{2j-1})) + C\Delta t\\ C\varepsilon_2^{-1}\mu^2(\mathcal{B}_2^l(x_{1i-1})\mathcal{B}_2^b(x_{2j-1})) + C\varepsilon_2^{-1}\mu^2(\mathcal{B}_2^l(x_{1i-1})\mathcal{B}_2^b(x_{2j-1})) + C\Delta t\end{pmatrix}.$$

Similarly, for $(x_{1i},x_{2j},t_k) \in [\tau_2,1)\times(0,\tau_2]\times(0,T]$, from (4.8) and Lemma 2.6, we can deduce

$$|\mathcal{L}^{N,N}_{\varepsilon,\mu}(\mathbf{S}_{lb}-\mathbf{s}_{lb})(x_{1i},x_{2j},t_k)| \leq \begin{pmatrix}C\varepsilon_1^{-1}\mu^2(\mathcal{B}_1^l(x_{1i-1})\mathcal{B}_1^b(x_{2j-1})) + C\varepsilon_2^{-1}\mu^2(\mathcal{B}_2^l(x_{1i-1})\mathcal{B}_2^b(x_{2j-1})) + C\Delta t\\ C\varepsilon_2^{-1}\mu^2(\mathcal{B}_2^l(x_{1i-1})\mathcal{B}_2^b(x_{2j-1})) + C\varepsilon_2^{-1}\mu^2(\mathcal{B}_2^l(x_{1i-1})\mathcal{B}_2^b(x_{2j-1})) + C\Delta t\end{pmatrix}.$$

By employing an appropriate barrier function for the corner layer component over the domain $0 \le i \le N, 0 \le j \le N, 0 \le k \le M$, we deduce that, for each component,

$$|(\mathbf{S}_{lb} - \mathbf{s}_{lb})(x_{1i}, x_{2j}, t_k)| \le C(N^{-1} + \Delta t),$$

which is the required result. □

In a similar manner, analogous bounds can be established for the errors associated with the remaining corner layer components $\mathbf{s}_{br}$, $\mathbf{s}_{rt}$, and $\mathbf{s}_{lt}$ in the case where $\vartheta\mu^2 > \Lambda\varepsilon_2$. Next, we proceed with the analysis of the second case, namely when $\vartheta\mu^2 \le \Lambda\varepsilon_1$.

Lemma 4.6. *Let* $\mathbf{s}_n$ *and* $\mathbf{S}_n$ *be the exact and numerical solutions of* (2.4) *and* (4.3)*, respectively, for* $n = lb, br, rt, lt$*. For* $\vartheta\mu^2 \le \Lambda\varepsilon_1$*, we have*

$$|\boldsymbol{S}_n(x_{1i}, x_{2j}, t_k) - \boldsymbol{s}_n(x_{1i}, x_{2j}, t_k)| \le C(N^{-1} + \Delta t).$$

Proof. If $\tau_1 = 1/8$ and $\tau_2 = 1/4$, the proof can be carried out by applying standard techniques on uniform meshes, taking into account that $\sqrt{\varepsilon_1} \le CN^{-1}$ and $\sqrt{\varepsilon_2} \le CN^{-1}$. Therefore, by employing (4.3) along with Theorem 2.6, we obtain

$$\begin{aligned}\|\boldsymbol{\mathcal{L}}^{N,N}_{\boldsymbol{\varepsilon},\boldsymbol{\mu}}(\mathbf{S}_{lb} - \mathbf{s}_{lb})\| &\le C\Big[\Delta t\Big\|\frac{\partial^2 \mathbf{s}_{lb}}{\partial t^2}\Big\| + (h_i + h_{i+1})\Big(\boldsymbol{\varepsilon}\Big\|\frac{\partial^3 \mathbf{s}_{lb}}{\partial {x_1}^3}\Big\| + \boldsymbol{\mu}\Big\|\frac{\partial^2 \mathbf{s}_{lb}}{\partial {x_1}^2}\Big\|\Big) + (k_j + k_{j+1})\Big(\boldsymbol{\varepsilon}\Big\|\frac{\partial^3 \mathbf{s}_{lb}}{\partial {x_2}^3}\Big\| + \boldsymbol{\mu}\Big\|\frac{\partial^2 \mathbf{s}_{lb}}{\partial {x_2}^2}\Big\|\Big)\Big]\\ &\le CN^{-1}.\end{aligned}$$

Further, if $\tau_1 = \sqrt{\dfrac{\varepsilon_1}{\Lambda\vartheta}}\ln N$, $\tau_2 = 1/4$, and we assume that $(x_{1i}, x_{2j}, t_k) \in (\tau_2, 1-\tau_2) \times (0,1) \times (0,T] \cup (\tau_1, \tau_2) \times (0,1) \times (0,T] \cup (0,\tau_1) \times (\tau_2, 1) \times (0,T] \cup (1-\tau_2, 1-\tau_1) \times (0,1) \times (0,T]$, then we have

$$|\boldsymbol{\mathcal{L}}^{N,N}_{\boldsymbol{\varepsilon},\boldsymbol{\mu}}(\vec{\mathbf{S}}_{lb} - \mathbf{s}_{lb})(x_{1i}, x_{2j}, t_k)| \le C\begin{pmatrix}\varepsilon_2^{-1/2}(\mathcal{B}^l_2(x_{1i-1})\mathcal{B}^b_2(x_{2j-1})) + \Delta t\\ \varepsilon_2^{-1/2}(\mathcal{B}^l_2(x_{1i-1})\mathcal{B}^b_2(x_{2j-1})) + \Delta t\end{pmatrix}.$$

When $(x_{1i}, x_{2j}, t_k) \in (0,\tau_1] \times (0,\tau_2] \times (0,T]$ or $[1-\tau_1, 1) \times (0,\tau_2] \times (0,T]$, it holds that

$$|\boldsymbol{\mathcal{L}}^{N,N}_{\boldsymbol{\varepsilon},\boldsymbol{\mu}}(\mathbf{S}_{lb} - \mathbf{s}_{lb})(x_{1i}, x_{2j}, t_k)| \le C\begin{pmatrix}\varepsilon_1^{-1/2} + \varepsilon_2^{-1/2} + \Delta t\\ \varepsilon_2^{-1/2} + \varepsilon_2^{-1/2} + \Delta t\end{pmatrix}.$$

If $\tau_2 = \sqrt{\dfrac{\varepsilon_2}{\Lambda\vartheta}}\ln N$ and $\tau_1 = \dfrac{\tau_2}{2}$, $\dfrac{\sqrt{\varepsilon_2}}{2} \le \sqrt{\varepsilon_1} < \sqrt{\varepsilon_2}$, hence $\tau_2 \le C\sqrt{\varepsilon_1}\ln N$.

By employing the barrier function from Lemma 4.2, the error estimate for the regions $(x_{1i}, x_{2j}, t_k) \in [\tau_2, 1-\tau_2] \times (0,1) \times (0,T]$, $(0,\tau_1] \times [\tau_2, 1) \times (0,T]$ and $[1-\tau_2, 1) \times [\tau_2, 1) \times (0,T]$ can be established as follows:

$$\begin{aligned}|(\mathbf{S}_{lb} - \mathbf{s}_{lb})(x_{1i}, x_{2j}, t_k)| &\le |\mathbf{S}_{lb}(x_{1i}, x_{2j}, t_k)| + |\mathbf{s}_{lb}(x_{1i}, x_{2j}, t_k)|\\ &\le C\min\{\mathcal{B}^{l,N}_2(\tau_2), \mathcal{B}^{b,N}_2(\tau_2)\} \le CN^{-1}.\end{aligned}$$

In order to obtain suitable bounds for the error in the region $(x_{1i}, x_{2j}, t_k) \in (\tau_1, \tau_2) \times (0, \tau_2) \times (0, T]$ or $(1-\tau_2, 1-\tau_1) \times (0, \tau_2) \times (0, T]$, along with the conditions $(h_i + h_{i+1}) \leq \sqrt{\varepsilon_1}$ and $(k_j + k_{j+1}) \leq \sqrt{\varepsilon_1}$, the following holds:

$$|\mathcal{L}_{\varepsilon,\mu}^{N,N}(\mathbf{S}_{lb} - \mathbf{s}_{lb})(x_{1i}, x_{2j}, t_k)| \leq C\sqrt{\varepsilon_1}\begin{pmatrix} \varepsilon_1^{-1/2} + \varepsilon_2^{-1/2} + \Delta t \\ \varepsilon_2^{-1/2} + \varepsilon_2^{-1/2} + \Delta t \end{pmatrix} \leq CN^{-1} + C\Delta t.$$

In the cases where (x_{1i}, x_{2j}, t_k) belongs to either $(0, \tau_1)\times(0, \tau_2)\times(0, T]$ or $(1-\tau_1, 1)\times(0, \tau_2)\times(0, T]$, we have $h_i + h_{i+1} \leq C\sqrt{\varepsilon_1},\ k_j + k_{j+1} \leq C\sqrt{\varepsilon_1}$. Using a similar analytical approach as previously described, the corresponding bounds are derived.

Assuming that $\tau_1 = \sqrt{\frac{\varepsilon_1}{\Lambda\vartheta\vartheta}}\ln N$ and $\tau_2 = \sqrt{\frac{\varepsilon_2}{\Lambda\vartheta}}\ln N$, and in cases where $(x_{1i}, x_{2j}, t_k) \in [\tau_2, 1-\tau_2] \times (0, 1) \times (0, T]$, $(0, \tau_1] \times (0, \tau_2) \times (0, T]$, or $(1-\tau_1, 1) \times (0, \tau_2) \times (0, T]$, the required bounds can be obtained using a similar approach as applied to the corresponding intervals in the previous cases. When (x_{1i}, x_{2j}, t_k) is within either $(\tau_1, \tau_2)\times(0, 1)\times(0, T]$ or $(1-\tau_2, 1-\tau_1)\times(0, 1)\times(0, T]$ or $(0, \tau_1)\times(\tau_2, 1)\times(0, T]$ or $(1-\tau_1, 1) \times (\tau_2, 1) \times (0, T]$, we have $h_i + h_{i+1} \leq CN^{-1}\tau_2 \leq C\sqrt{\varepsilon_2}$. Consequently, we obtain

$$|\mathcal{L}_{\varepsilon,\mu}^{N,N}(\mathbf{S}_{lb} - \mathbf{s}_{lb})(x_{1i}, x_{2j}, t_k)| \leq C(N^{-1} + \Delta t).$$

□

Analogously, similar error bounds are obtained for the remaining corner layers $\mathbf{s}_{br}$, $\mathbf{s}_{rt}$, and $\mathbf{s}_{lt}$ in the case $\vartheta\mu^2 \leq \Lambda\varepsilon_1$. Finally, we analyze the third case when $\Lambda\varepsilon_1 < \vartheta\mu^2 < \Lambda\varepsilon_2$.

Lemma 4.7. *Let $\mathbf{s}_n$ and $\mathbf{S}_n$ be the true and numerical solutions of* (2.4) *and (4.3), respectively, for $n = lb, br, rt, lt$. For $\Lambda\varepsilon_1 < \vartheta\mu^2 < \Lambda\varepsilon_2$, we have*

$$|\mathbf{S}_n(x_{1i}, x_{2j}, t_k) - \mathbf{s}_n(x_{1i}, x_{2j}, t_k)| \leq C(N^{-1} + \Delta t).$$

Proof. Using similar arguments as presented in Lemmas 4.4, 4.5, and 4.6, the error estimates for the intermediate case $\Lambda\varepsilon_1 < \vartheta\mu^2 < \Lambda\varepsilon_2$ can also be established. □

By combining all the previous results, we arrive at the main result of this work.

Theorem 4.8. *Let $\mathbf{z}$ and $\mathbf{Z}$ denote the exact and continuous solutions of* (1.1) *and* (3.4)*, respectively, on the constructed BS mesh. Then, the error satisfies the following estimate:*

$$|\mathbf{Z}(x_{1i}, x_{2j}, t_k) - z(x_{1i}, x_{2j}, t_k)| \leq C(N^{-1} + \Delta t), \tag{4.13}$$

and therefore, the proposed numerical scheme achieves first-order uniform convergence.

5. Numerical experiments

Section 3 describes the implementation of our algorithm on the BS mesh. To show the effectiveness of the numerical approach, two test problems of the form (1.1) are considered. All numerical experiments are performed in MATLAB R2024a on a system with 32 GB RAM and an Intel i5 processor (1.8 GHz). Due to the complexity of the considered problems, the computation time required to obtain accurate results is relatively high. However, to enhance computational efficiency and minimize memory usage, the algorithm utilizes sparse matrix techniques to solve the resulting linear systems.

To address the test problems, the numerical solutions are arranged in the following form:

$$\text{(initialize)} Z_1(x_{1i}, x_{2j}, t_0) = [\psi_1]_{\Omega^N}, \tag{5.1}$$

$$Z_2(x_{1i}, x_{2j}, t_0) = [\psi_2]_{\Omega^N}, \tag{5.2}$$

$$Z = \begin{cases} \text{For } m = 1, 2, \ldots, M, \\ Z_1(x_{10}, x_{20}, t_m), Z_1(x_{11}, x_{20}, t_m), \ldots, Z_1(x_{1N}, x_{20}, t_m), \\ Z_1(x_{10}, x_{21}, t_m), Z_1(x_{11}, x_{21}, t_m), \ldots, Z_1(x_{1N}, x_{21}, t_m), \\ Z_1(x_{10}, x_{22}, t_m), Z_1(x_{11}, x_{22}, t_m), \ldots, Z_1(x_{1N}, x_{22}, t_m), \\ \cdots\cdots\cdots\cdots\cdots\cdots\cdots\cdots\cdots\cdots \\ Z_1(x_{10}, x_{2N}, t_m), Z_1(x_{11}, x_{2N}, t_m), \ldots, Z_1(x_{1N}, x_{2N}, t_m), \\ Z_2(x_{10}, x_{20}, t_m), Z_2(x_{11}, x_{20}, t_m), \ldots, Z_2(x_{1N}, x_{20}, t_m), \\ Z_2(x_{10}, x_{21}, t_m), Z_2(x_{11}, x_{21}, t_m), \ldots, Z_2(x_{1N}, x_{21}, t_m), \\ \cdots\cdots\cdots\cdots\cdots\cdots\cdots\cdots\cdots\cdots \\ Z_2(x_{10}, x_{2N}, t_m), Z_2(x_{11}, x_{2N}, t_m), \ldots, Z_2(x_{1N}, x_{2N}, t_m), \end{cases} \tag{5.3}$$

where the values $Z_n(x_{1_0}, x_{2_j}, t_m)$, $Z_n(x_{1_i}, x_{2_0}, t_m)$, $Z_n(x_{1_N}, x_{2_j}, t_m)$, and $Z_n(x_{1_i}, x_{2_N}, t_m)$, for $n = 1, 2,\ i, j = 0, \ldots, N,\ m = 1, \ldots, M$, are determined from the prescribed boundary conditions.

Then, the resulting linear system can be written as $[A]^m_{(2(N+1)^2, 2(N+1)^2)}[Z]^m_{(2(N+1)^2,1)} = [F]^m_{(2(N+1)^2,1)}$, for $m = 1, \ldots M$, and we solve this system by using MATLAB, taking into account that the matrix A is sparse.

In this section, we solve with our method (3.4) two test examples of problems of type (1.1). The data of the first example are given by

Example 5.1.

$$\frac{\partial z}{\partial t} - \boldsymbol{\varepsilon}\left(\frac{\partial^2 z}{\partial {x_1}^2} + \frac{\partial^2 z}{\partial {x_2}^2}\right) + \boldsymbol{\mu}\left(\boldsymbol{A}_1(x_1, x_2, t)\frac{\partial z}{\partial x_1} + \boldsymbol{A}_2(x_1, x_2, t)\frac{\partial z}{\partial x_2}\right) + \boldsymbol{B}(x_1, x_2, t)\boldsymbol{z} = \boldsymbol{f}(x_1, x_2, t),\ \forall (x_1, x_2, t) \in \Omega \times (0, T],$$

where the boundary conditions as well as convection, reaction coefficients, and source terms are given by

$$\boldsymbol{z}(x_1, 0, t) = \boldsymbol{z}(x_1, 1, t) = \boldsymbol{z}(0, x_2, t) = \boldsymbol{z}(1, x_2, t) = \boldsymbol{z}(x_1, x_2, 0) = 0,$$

$$\boldsymbol{A}_1(x_1, x_2, t)\begin{pmatrix} 1 + x_1 x_2 & 0 \\ 0 & 2 - x_1 x_2 \end{pmatrix}, \boldsymbol{A}_2(x_1, x_2, t) = \begin{pmatrix} 2 + \sin(x_1 + x_2) & 0 \\ 0 & 2 - \cos(x_1 + x_2) \end{pmatrix},$$

$$\boldsymbol{B}(x_1, x_2, t) = \begin{pmatrix} (3 + x_1 x_2)\exp(-t) & -1 - {x_1}^2 {x_2}^2 \\ -1 - \exp(x_1 x_2) & (3 + \exp(x_1 x_2))(1 - 2\exp(-t)) \end{pmatrix},$$

$$\boldsymbol{f}(x_1, x_2, t) = \Big(\exp(-x_1 - x_2)\sin(\pi t), \exp(-x_1 - x_2)\cos(\pi t/2)\Big)^T,$$

with $T = 1$. The data of the second example are

Example 5.2.

$$\frac{\partial z}{\partial t} - \boldsymbol{\varepsilon}\Big(\frac{\partial^2 z}{\partial {x_1}^2} + \frac{\partial^2 z}{\partial {x_2}^2}\Big) + \boldsymbol{\mu}\Big(\boldsymbol{A}_1(x_1,x_2,t)\frac{\partial z}{\partial x_1} + \boldsymbol{A}_2(x_1,x_2,t)\frac{\partial z}{\partial x_2}\Big) + \boldsymbol{B}(x_1,x_2,t)\boldsymbol{z} = \boldsymbol{f}(x_1,x_2,t),\ \forall(x_1,x_2,t) \in \Omega \times (0,T],$$

where now the boundary conditions as well as convection, reaction coefficients, and source terms are given by

$$\boldsymbol{z}(x_1,x_2,t) = \Big(x_1(1-x_1)x_2(1-x_2)(1-exp(-5t)), x_1(1-x_1)x_2(1-x_2)(1-exp(-t))\Big)^T, (x_1,x_2,t) \in \partial\Omega \times [0,T],$$

$$\boldsymbol{z}(x_1,x_2,0) = \boldsymbol{0},$$

$$\boldsymbol{A}_1(x_1,x_2,t) = \begin{pmatrix} 1 + x_1x_2(1-\exp(-t)) & 0 \\ 0 & 1 - x_1x_2(1-\exp(-2t)) \end{pmatrix}, \boldsymbol{A}_2(x_1,x_2,t) = \begin{pmatrix} 2+\exp(x_1x_2) & 0 \\ 0 & 2 - exp(x_1x_2) \end{pmatrix},$$

$$\boldsymbol{B}(x_1,x_2,t) = \begin{pmatrix} (3 + {x_1}^2{x_2}^2)(1-\exp(-t)) & -1 - x_1x_2 \\ -1-\exp(x_1x_2) & (3+\exp(x_1x_2))(1-2\exp(-t)) \end{pmatrix},$$

$$\boldsymbol{f}(x_1,x_2,t) = \Big(\sin(\pi x_1x_2)\sin(\pi t), \cos(\pi x_1x_2/2)\cos(\pi t/2)\Big)^T,$$

also with $T = 1$. Note that in this second example, the coefficients of the convection matrix A_1 depend also on the time variable; then, from a numerical point of view, we see that our numerical algorithm can be used efficiently for more general problems that this one in (1.1).

Figures 2–4 and 5–7 illustrate the two components of the numerical solution for Examples 5.1 and 5.2, respectively, obtained for different values of the diffusion and convection parameters ε_1, ε_2, and μ while keeping the discretization parameters N and M fixed at the final time $T = 1$. These figures clearly reveal the presence of boundary layers in the numerical solution.

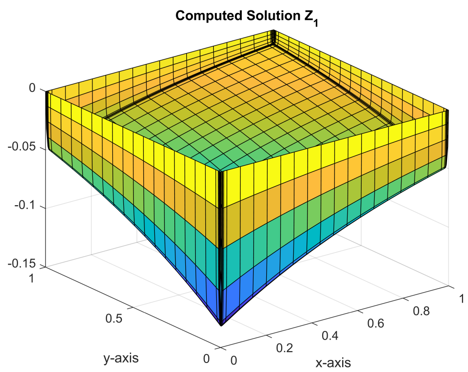

(a) Surface graph of the numerical solution z_1;

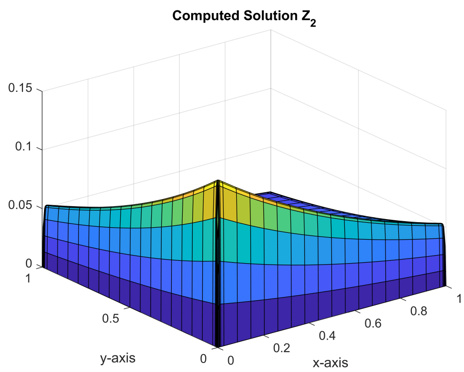

(b) surface graph of the numerical solution z_2.

Figure 2. When $\varepsilon_1 = 5^{-6}10^{-2}, \varepsilon_2 = 5^{-4}10^{-2}$, $\mu^2 = 5^{-8}10^{-2}, N = 32$, and $M = 16$ for Example 5.1.

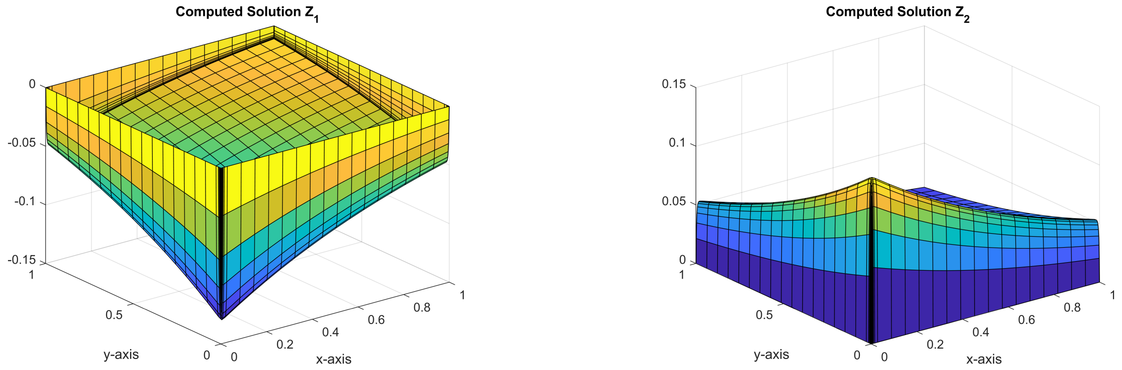

(a) Surface graph of the numerical solution z_1.

(b) surface graph of the numerical solution z_2.

Figure 3. When $\varepsilon_1 = 5^{-8}10^{-2}, \varepsilon_2 = 5^{-6}10^{-2}, \mu^2 = 5^{-4}10^{-2}, N = 32$, and $M = 16$ for Example 5.1.

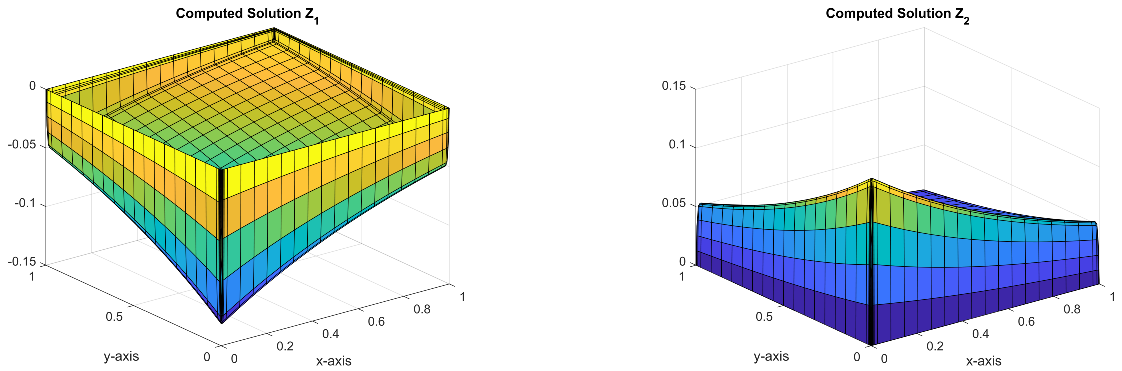

(a) Surface graph of the numerical solution z_1;

(b) surface graph of the numerical solution z_2.

Figure 4. When $\varepsilon_1 = 5^{-8}10^{-2}, \varepsilon_2 = 5^{-4}10^{-2}, \mu^2 = 5^{-6}10^{-2}, N = 32$, and $M = 16$ for Example 5.1.

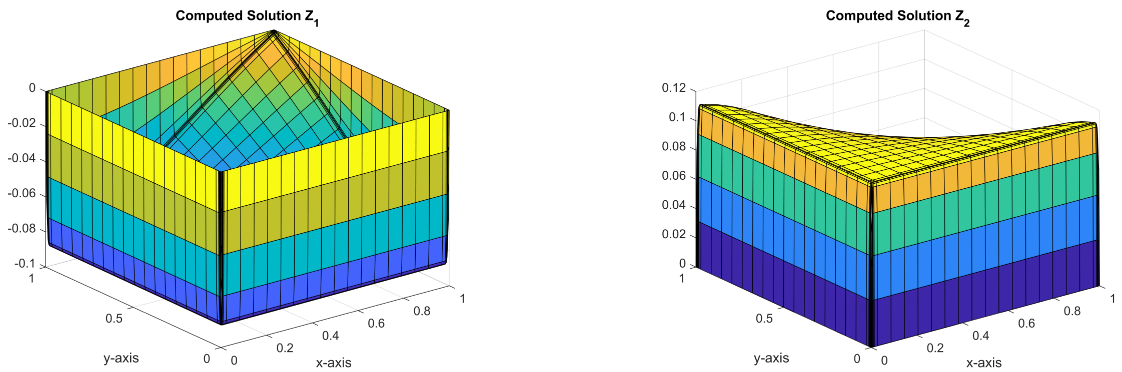

(a) Surface graph of the numerical solution z_1;

(b) surface graph of the numerical solution z_2.

Figure 5. When $\varepsilon_1 = 5^{-6}10^{-2}, \varepsilon_2 = 5^{-4}10^{-2}, \mu^2 = 5^{-8}10^{-2}, N = 32$, and $M = 16$ for Example 5.2.

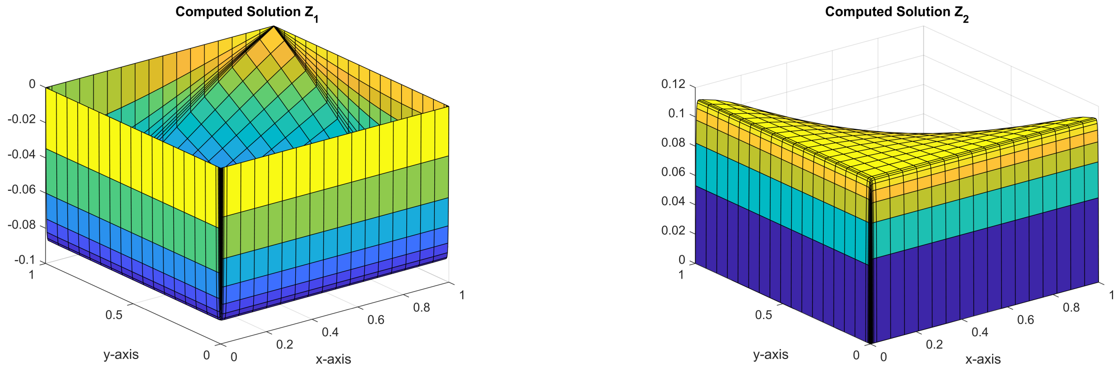

(a) Surface graph of the numerical solution z_1; **(b)** surface graph of the numerical solution z_2.

Figure 6. When $\varepsilon_1 = 5^{-8}10^{-2}, \varepsilon_2 = 5^{-6}10^{-2}$, $\mu^2 = 5^{-4}10^{-2}, N = 32$, and $M = 16$ for Example 5.2.

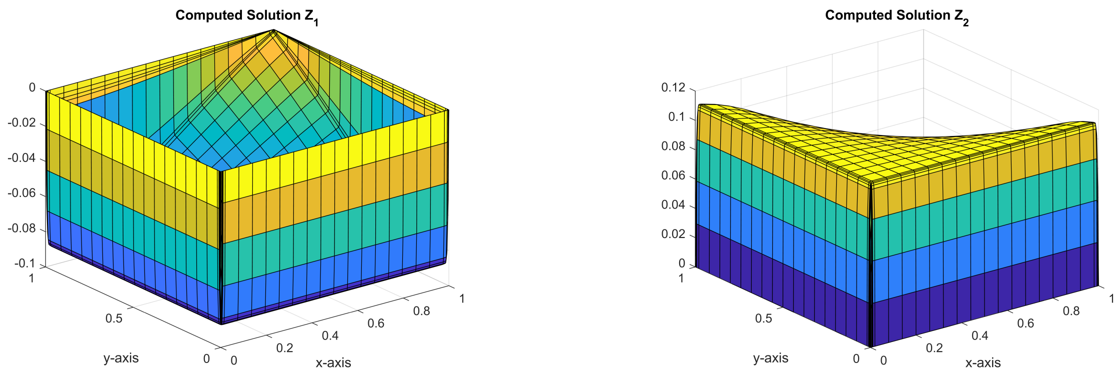

(a) Surface graph of the numerical solution z_1; **(b)** surface graph of the numerical solution z_2.

Figure 7. When $\varepsilon_1 = 5^{-8}10^{-2}, \varepsilon_2 = 5^{-4}10^{-2}$, $\mu^2 = 5^{-6}10^{-2}, N = 32$, and $M = 16$ for Example 5.2.

As the exact solution of this problem is unknown, to approximate the maximum point-wise errors, we use, in a usual way, the double mesh technique (see [13]). Then, we calculate

$$E_{\varepsilon,\mu}^{N,M} = \max_{(x_i,y_j,t_n)\in\overline{Q}^{N,M}} |\widehat{Z}^{2N,2M}(x_{12i}, x_{22j}, t_{2n}) - Z^{N,N}(x_{1i}, x_{2j}, t_n)|,$$

where $\widehat{Z}^{2N,2M}$ is the numerical solution obtained on a mesh with $2N$ subintervals in space and $2M$ subintervals in time, taking the mesh points of the coarse mesh and also their midpoints on each spatial and temporal direction. Then, the parameter uniform maximum point-wise errors are calculated applying the formula

$$E^{N,M} = \max_{\varepsilon,\mu} E_{\varepsilon,\mu}^{N,N}.$$

From the previous values, the uniform numerical orders of convergence are given by

$$Q^{N,M} = \log_2\left(\frac{E^{N,M}}{E^{2N,2M}}\right).$$

Tables 1, 3, and 5 show the maximum errors for the first component under various choices of the convection and diffusion parameter, together with selected discretization parameters N and M. These tables also report the maximum uniform errors along with the associated uniform orders of convergence. Similarly, Tables 2, 4, and 6 show the results for the second component for the same set of parameters. In an analogous manner, Tables 7, 8, 9, 10, 11, and 12 summarize the maximum errors and the numerical orders of convergence for the first and second components, corresponding to example 5.2.

The collection of results in Tables 1–12 clearly show the effectiveness of the proposed method, implemented on a BS mesh, in delivering accurate and efficient solutions for the test problems 5.1 and 5.2 across the three distinct ratios of diffusion to convection parameters.

Finally, Tables 13–15 present a comparison of the maximum point-wise errors $E^{N,M}$ and orders of convergence $Q^{N,M}$ for Example 5.1 under each of the cases, using the BS mesh and the standard Shishkin (S) mesh. As the mesh is refined, the errors decrease for both meshes, indicating the uniform convergence of the numerical scheme. However, for all grid levels and for both solution components z_1 and z_2, the BS mesh yields significantly smaller errors than the S mesh and achieves near first-order convergence. This clearly permits us to conclude the superior accuracy and parameter-uniform convergence of the BS mesh compared to the standard S mesh.

Table 1. When $\vartheta\mu^2 \leq \Lambda\varepsilon_1 \leq \Lambda\varepsilon_2$.

First component z_1					
$\varepsilon_1 = 5^{-6}\eta$ $\varepsilon_2 = 5^{-4}\eta$ $\mu^2 = 5^{-8}\eta$					
M η/N	16 32	32 64	64 128	128 256	256 512
10^{-1}	4.963e-3	3.061e-3	1.678e-3	8.764e-4	4.473e-4
10^{-2}	4.994e-3	3.087e-3	1.696e-3	8.875e-4	4.539e-4
10^{-3}	5.004e-3	3.095e-3	1.701e-3	8.910e-4	4.561e-4
10^{-4}	5.007e-3	3.098e-3	1.703e-3	8.921e-4	4.567e-4
10^{-5}	5.008e-3	3.099e-3	1.704e-3	8.925e-4	4.569e-4
10^{-6}	5.008e-3	3.099e-3	1.704e-3	8.926e-4	4.570e-4
10^{-7}	5.008e-3	3.099e-3	1.704e-3	8.926e-4	4.570e-4
10^{-8}	5.008e-3	3.099e-3	1.704e-3	8.927e-4	4.570e-4
$E^{N,M}$	5.008e-3	3.099e-3	1.704e-3	8.927e-4	4.570e-4
$Q^{N,M}$	0.6924	0.8629	0.9327	0.9660	–

Table 2. When $\vartheta\mu^2 \leq \Lambda\varepsilon_1 \leq \Lambda\varepsilon_2$.

Second component z_2					
$\varepsilon_1 = 5^{-6}\eta$ $\varepsilon_2 = 5^{-4}\eta$ $\mu^2 = 5^{-8}\eta$					
M η/N	16 32	32 64	64 128	128 256	256 512
10^{-1}	4.988e-3	3.076e-3	1.685e-3	8.802e-4	4.492e-4
10^{-2}	5.019e-3	3.101e-3	1.703e-3	8.913e-4	4.559e-4
10^{-3}	5.029e-3	3.110e-3	1.709e-3	8.949e-4	4.580e-4
10^{-4}	5.033e-3	3.112e-3	1.711e-3	8.960e-4	4.587e-4
10^{-5}	5.034e-3	3.113e-3	1.711e-3	8.964e-4	4.589e-4
10^{-6}	5.034e-3	3.113e-3	1.711e-3	8.965e-4	4.590e-4
10^{-7}	5.034e-3	3.113e-3	1.711e-3	8.965e-4	4.590e-4
10^{-8}	5.034e-3	3.113e-3	1.711e-3	8.965e-4	4.590e-4
$E^{N,M}$	5.034e-3	3.113e-3	1.711e-3	8.965e-4	4.590e-4
$Q^{N,M}$	0.6934	0.8635	0.9325	0.9658	–

Tables 1 and 2 present the maximum point-wise errors $E^{N,M}$ and the corresponding numerical orders of convergence $Q^{N,M}$ for Example 5.1 when $\vartheta\mu^2 \leq \Lambda\varepsilon_1 \leq \Lambda\varepsilon_2$.

Table 3. When $\vartheta\mu^2 > \Lambda\varepsilon_2 \geq \Lambda\varepsilon_1$.

First component z_1					
$\varepsilon_1 = 5^{-8}\eta$	$\varepsilon_2 = 5^{-6}\eta$	$\mu^2 = 5^{-4}\eta$			
M	16	32	64	128	256
η/N	32	64	128	256	512
10^{-1}	1.042e-2	6.715e-3	4.150e-3	2.396e-3	1.316e-3
10^{-2}	1.043e-2	6.720e-3	4.152e-3	2.396e-3	1.316e-3
10^{-3}	1.044e-2	6.721e-3	4.152e-3	2.396e-3	1.316e-3
10^{-4}	1.044e-2	6.722e-3	4.152e-3	2.396e-3	1.316e-3
10^{-5}	1.044e-2	6.722e-3	4.152e-3	2.396e-3	1.316e-3
10^{-6}	1.044e-2	6.722e-3	4.152e-3	2.396e-3	1.316e-3
10^{-7}	1.044e-2	6.722e-3	4.152e-3	2.396e-3	1.316e-3
10^{-8}	1.044e-2	6.722e-3	4.152e-3	2.396e-3	1.316e-3
$E^{N,M}$	1.044e-2	6.722e-3	4.152e-3	2.396e-3	1.316e-3
$Q^{N,M}$	0.6352	0.6951	0.7932	0.8645	–

Table 4. When $\vartheta\mu^2 > \Lambda\varepsilon_2 \geq \Lambda\varepsilon_1$.

Second component z_2					
$\varepsilon_1 = 5^{-8}\eta$	$\varepsilon_2 = 5^{-6}\eta$	$\mu^2 = 5^{-4}\eta$			
M	16	32	64	128	256
η/N	32	64	128	256	512
10^{-1}	1.031e-2	6.641e-3	4.102e-3	2.367e-3	1.298e-3
10^{-2}	1.033e-2	6.646e-3	4.104e-3	2.367e-3	1.298e-3
10^{-3}	1.033e-2	6.648e-3	4.104e-3	2.367e-3	1.298e-3
10^{-4}	1.033e-2	6.648e-3	4.105e-3	2.368e-3	1.298e-3
10^{-5}	1.033e-2	6.648e-3	4.105e-3	2.368e-3	1.298e-3
10^{-6}	1.033e-2	6.648e-3	4.105e-3	2.368e-3	1.298e-3
10^{-7}	1.033e-2	6.648e-3	4.105e-3	2.368e-3	1.298e-3
10^{-8}	1.033e-2	6.648e-3	4.105e-3	2.368e-3	1.298e-3
$E^{N,M}$	1.033e-2	6.648e-3	4.105e-3	2.368e-3	1.298e-3
$Q^{N,M}$	0.6358	0.6955	0.7937	0.8674	–

Tables 3 and 4 present the maximum point-wise errors $E^{N,M}$ and the corresponding numerical orders of convergence $Q^{N,M}$ for Example 5.1 when $\vartheta\mu^2 > \Lambda\varepsilon_2 \geq \Lambda\varepsilon_1$.

Table 5. When $\Lambda\varepsilon_1 < \vartheta\mu^2 < \Lambda\varepsilon_2$.

First component z_1					
$\varepsilon_1 = 5^{-8}\eta$	$\varepsilon_2 = 5^{-4}\eta$	$\mu^2 = 5^{-6}\eta$			
M	16	32	64	128	256
η/N	32	64	128	256	512
10^{-1}	2.991e-3	1.778e-3	9.969e-4	5.361e-4	2.834e-4
10^{-2}	3.020e-3	1.794e-3	1.008e-3	5.433e-4	2.879e-4
10^{-3}	3.029e-3	1.799e-3	1.012e-3	5.457e-4	2.893e-4
10^{-4}	3.032e-3	1.800e-3	1.013e-3	5.464e-4	2.898e-4
10^{-5}	3.033e-3	1.801e-3	1.013e-3	5.466e-4	2.899e-4
10^{-6}	3.033e-3	1.801e-3	1.013e-3	5.467e-4	2.900e-4
10^{-7}	3.033e-3	1.801e-3	1.013e-3	5.467e-4	2.900e-4
10^{-8}	3.033e-3	1.801e-3	1.013e-3	5.467e-4	2.900e-4
$E^{N,M}$	3.033e-3	1.801e-3	1.013e-3	5.467e-4	2.900e-4
$Q^{N,M}$	0.7519	0.8302	0.8898	0.9147	–

Table 6. When $\Lambda\varepsilon_1 < \vartheta\mu^2 < \Lambda\varepsilon_2$

Second component z_2					
$\varepsilon_1 = 5^{-8}\eta$	$\varepsilon_2 = 5^{-4}\eta$	$\mu^2 = 5^{-6}\eta$			
M	16	32	64	128	256
η/N	32	64	128	256	512
10^{-1}	2.975e-3	1.812e-3	1.015e-3	5.455e-4	2.884e-4
10^{-2}	3.004e-3	1.827e-3	1.026e-3	5.528e-4	2.928e-4
10^{-3}	3.013e-3	1.832e-3	1.029e-3	5.551e-4	2.943e-4
10^{-4}	3.016e-3	1.834e-3	1.031e-3	5.559e-4	2.948e-4
10^{-5}	3.017e-3	1.834e-3	1.031e-3	5.561e-4	2.949e-4
10^{-6}	3.017e-3	1.835e-3	1.031e-3	5.562e-4	2.949e-4
10^{-7}	3.017e-3	1.835e-3	1.031e-3	5.562e-4	2.950e-4
10^{-8}	3.017e-3	1.835e-3	1.031e-3	5.562e-4	2.950e-4
$E^{N,M}$	3.017e-3	1.835e-3	1.031e-3	5.562e-4	2.950e-4
$Q^{N,M}$	0.7173	0.8317	0.8904	0.9149	–

Tables 5 and 6 present the maximum point-wise errors $E^{N,M}$ and the corresponding numerical orders of convergence $Q^{N,M}$ for Example 5.1 when $\Lambda\varepsilon_1 < \vartheta\mu^2 < \Lambda\varepsilon_2$.

Table 7. When $\vartheta\mu^2 \leq \Lambda\varepsilon_1 \leq \Lambda\varepsilon_2$.

First component z_1					
$\varepsilon_1 = 5^{-6}\eta$	$\varepsilon_2 = 5^{-4}\eta$	$\mu^2 = 5^{-8}\eta$			
M	16	32	64	128	256
η/N	32	64	128	256	512
10^{-1}	3.462e-3	1.802e-3	8.450e-4	3.841e-4	1.709e-4
10^{-2}	3.466e-3	1.806e-3	8.451e-4	3.841e-4	1.709e-4
10^{-3}	3.468e-3	1.808e-3	8.451e-4	3.841e-4	1.709e-4
10^{-4}	3.468e-3	1.808e-3	8.451e-4	3.841e-4	1.709e-4
10^{-5}	3.468e-3	1.808e-3	8.451e-4	3.841e-4	1.709e-4
10^{-6}	3.468e-3	1.808e-3	8.451e-4	3.841e-4	1.709e-4
10^{-7}	3.468e-3	1.808e-3	8.451e-4	3.841e-4	1.709e-4
10^{-8}	3.468e-3	1.808e-3	8.451e-4	3.841e-4	1.709e-4
$E^{N,M}$	3.468e-3	1.808e-3	8.451e-4	3.841e-4	1.709e-4
$Q^{N,M}$	0.9397	1.0972	1.1376	1.1683	–

Table 8. When $\vartheta\mu^2 \leq \Lambda\varepsilon_1 \leq \Lambda\varepsilon_2$.

Second component z_2					
$\varepsilon_1 = 5^{-6}\eta$	$\varepsilon_2 = 5^{-4}\eta$	$\mu^2 = 5^{-8}\eta$			
M	16	32	64	128	256
η/N	32	64	128	256	512
10^{-1}	3.518e-3	1.830e-3	8.592e-4	3.905e-4	1.737e-4
10^{-2}	3.523e-3	1.835e-3	8.592e-4	3.905e-4	1.737e-4
10^{-3}	3.524e-3	1.837e-3	8.592e-4	3.905e-4	1.737e-4
10^{-4}	3.524e-3	1.837e-3	8.592e-4	3.905e-4	1.737e-4
10^{-5}	3.525e-3	1.837e-3	8.592e-4	3.905e-4	1.737e-4
10^{-6}	3.525e-3	1.837e-3	8.592e-4	3.905e-4	1.737e-4
10^{-7}	3.525e-3	1.837e-3	8.592e-4	3.905e-4	1.737e-4
10^{-8}	3.525e-3	1.837e-3	8.592e-4	3.905e-4	1.737e-4
$E^{N,M}$	3.525e-3	1.837e-3	8.592e-4	3.905e-4	1.737e-4
$Q^{N,M}$	0.9403	1.0963	1.1377	1.1687	–

Tables 7 and 8 present the maximum point-wise errors $E^{N,M}$ and the corresponding numerical orders of convergence $Q^{N,M}$ for Example 5.2 when $\vartheta\mu^2 \leq \Lambda\varepsilon_1 \leq \Lambda\varepsilon_2$.

Table 9. When $\vartheta\mu^2 > \Lambda\varepsilon_2 \geq \Lambda\varepsilon_1$.

First component z_1					
$\varepsilon_1 = 5^{-8}\eta$	$\varepsilon_2 = 5^{-6}\eta$	$\mu^2 = 5^{-4}\eta$			
M	16	32	64	128	256
η/N	32	64	128	256	512
10^{-1}	7.740e-3	5.216e-3	3.212e-3	1.873e-3	1.024e-3
10^{-2}	7.741e-3	5.217e-3	3.215e-3	1.874e-3	1.026e-3
10^{-3}	7.742e-3	5.218e-3	3.218e-3	1.875e-3	1.028e-3
10^{-4}	7.742e-3	5.218e-3	3.218e-3	1.875e-3	1.028e-3
10^{-5}	7.742e-3	5.218e-3	3.218e-3	1.875e-3	1.028e-3
10^{-6}	7.742e-3	5.218e-3	3.218e-3	1.875e-3	1.028e-3
10^{-7}	7.742e-3	5.218e-3	3.218e-3	1.875e-3	1.028e-3
10^{-8}	7.742e-3	5.218e-3	3.218e-3	1.875e-3	1.028e-3
$E^{N,M}$	7.742e-3	5.218e-3	3.218e-3	1.875e-3	1.028e-3
$Q^{N,M}$	0.5692	0.6973	0.7793	0.8671	–

Table 10. When $\vartheta\mu^2 > \Lambda\varepsilon_2 \geq \Lambda\varepsilon_1$.

Second component z_2					
$\varepsilon_1 = 5^{-8}\eta$	$\varepsilon_2 = 5^{-6}\eta$	$\mu^2 = 5^{-4}\eta$			
M	16	32	64	128	256
η/N	32	64	128	256	512
10^{-1}	7.708e-3	5.186e-3	3.201e-3	1.857e-3	1.016e-3
10^{-2}	7.710e-3	5.188e-3	3.203e-3	1.859e-3	1.018e-3
10^{-3}	7.710e-3	5.188e-3	3.203e-3	1.859e-3	1.018e-3
10^{-4}	7.710e-3	5.188e-3	3.203e-3	1.859e-3	1.018e-3
10^{-5}	7.710e-3	5.188e-3	3.203e-3	1.859e-3	1.018e-3
10^{-6}	7.710e-3	5.188e-3	3.203e-3	1.859e-3	1.018e-3
10^{-7}	7.710e-3	5.188e-3	3.203e-3	1.859e-3	1.018e-3
10^{-8}	7.710e-3	5.188e-3	3.203e-3	1.859e-3	1.018e-3
$E^{N,M}$	7.710e-3	5.188e-3	3.203e-3	1.859e-3	1.018e-3
$Q^{N,M}$	0.5716	0.6958	0.7849	0.8688	–

Tables 9 and 10 present the maximum point-wise errors $E^{N,M}$ and the corresponding numerical orders of convergence $Q^{N,M}$ for Example 5.2 when $\vartheta\mu^2 > \Lambda\varepsilon_2 \geq \Lambda\varepsilon_1$.

Table 11. When $\Lambda\varepsilon_1 < \vartheta\mu^2 < \Lambda\varepsilon_2$.

First component z_1					
$\varepsilon_1 = 5^{-8}\eta$	$\varepsilon_2 = 5^{-4}\eta$	$\mu^2 = 5^{-6}\eta$			
M	16	32	64	128	256
η/N	32	64	128	256	512
10^{-1}	1.921e-3	9.864e-4	4.878e-4	2.381e-4	1.209e-4
10^{-2}	1.921e-3	9.864e-4	4.879e-4	2.397e-4	1.217e-4
10^{-3}	1.921e-3	9.864e-4	4.879e-4	2.402e-4	1.220e-4
10^{-4}	1.921e-3	9.864e-4	4.879e-4	2.403e-4	1.221e-4
10^{-5}	1.921e-3	9.864e-4	4.879e-4	2.404e-4	1.221e-4
10^{-6}	1.921e-3	9.864e-4	4.879e-4	2.404e-4	1.221e-4
10^{-7}	1.921e-3	9.864e-4	4.879e-4	2.404e-4	1.221e-4
10^{-8}	1.921e-3	9.864e-4	4.879e-4	2.404e-4	1.221e-4
$E^{N,M}$	1.921e-3	9.864e-4	4.879e-4	2.404e-4	1.221e-4
$Q^{N,M}$	0.9616	1.0156	1.0211	0.9774	–

Table 12. When $\Lambda\varepsilon_1 < \vartheta\mu^2 < \Lambda\varepsilon_2$.

Second component z_2					
$\varepsilon_1 = 5^{-8}\eta$	$\varepsilon_2 = 5^{-6}\eta$	$\mu^2 = 5^{-4}\eta$			
M	16	32	64	128	256
η/N	32	64	128	256	512
10^{-1}	7.708e-3	5.186e-3	3.201e-3	1.857e-3	1.016e-3
10^{-2}	7.710e-3	5.188e-3	3.203e-3	1.859e-3	1.018e-3
10^{-3}	7.710e-3	5.188e-3	3.203e-3	1.859e-3	1.018e-3
10^{-4}	7.710e-3	5.188e-3	3.203e-3	1.859e-3	1.018e-3
10^{-5}	7.710e-3	5.188e-3	3.203e-3	1.859e-3	1.018e-3
10^{-6}	7.710e-3	5.188e-3	3.203e-3	1.859e-3	1.018e-3
10^{-7}	7.710e-3	5.188e-3	3.203e-3	1.859e-3	1.018e-3
10^{-8}	7.710e-3	5.188e-3	3.203e-3	1.859e-3	1.018e-3
$E^{N,M}$	7.710e-3	5.188e-3	3.203e-3	1.859e-3	1.018e-3
$Q^{N,M}$	0.5716	0.6958	0.7849	0.8688	–

Tables 11 and 12 present the maximum point-wise errors $E^{N,M}$ and the corresponding numerical orders of convergence $Q^{N,M}$ for Example 5.2 when $\Lambda\varepsilon_1 < \vartheta\mu^2 < \Lambda\varepsilon_2$.

Table 13. For Example 5.1, maximum point-wise errors $E^{N,M}$ and orders of convergence $Q^{N,M}$ when $\vartheta\mu^2 \leq \Lambda\varepsilon_1 \leq \Lambda\varepsilon_2$.

(N, M)	First Component z_1				Second Component z_2			
	BS mesh		S mesh		BS mesh		S mesh	
	$E^{N,M}$	$Q^{N,M}$	$E^{N,M}$	$Q^{N,M}$	$E^{N,M}$	$Q^{N,M}$	$E^{N,M}$	$Q^{N,M}$
32, 16	5.008×10^{-3}	0.6924	1.232×10^{-2}	0.4402	5.034×10^{-3}	0.6934	1.446×10^{-2}	0.6639
64, 32	3.099×10^{-3}	0.8629	9.080×10^{-3}	0.6753	3.113×10^{-3}	0.8635	9.127×10^{-3}	0.7844
128, 64	1.704×10^{-3}	0.9327	5.686×10^{-3}	0.8489	1.711×10^{-3}	0.9325	5.299×10^{-3}	0.7735
256, 128	8.927×10^{-4}	0.9960	3.157×10^{-3}	0.8853	8.965×10^{-4}	0.9658	3.100×10^{-3}	0.8950
512, 256	4.570×10^{-4}	–	1.745×10^{-3}	–	4.590×10^{-4}	–	1.667×10^{-3}	–

Table 14. For Example 5.1, maximum point-wise errors $E^{N,M}$ and orders of convergence $Q^{N,M}$ when $\vartheta\mu^2 > \Lambda\varepsilon_2 \geq \Lambda\varepsilon_1$.

(N, M)	First Component z_1				Second Component z_2			
	BS mesh		S mesh		BS mesh		S mesh	
	$E^{N,M}$	$Q^{N,M}$	$E^{N,M}$	$Q^{N,M}$	$E^{N,M}$	$Q^{N,M}$	$E^{N,M}$	$Q^{N,M}$
32, 16	1.044×10^{-2}	0.6352	1.822×10^{-2}	0.3801	1.033×10^{-2}	0.6358	1.805×10^{-2}	0.3790
64, 32	6.722×10^{-3}	0.6951	1.400×10^{-2}	0.3624	6.648×10^{-3}	0.6955	1.388×10^{-2}	0.3647
128, 64	4.152×10^{-3}	0.7932	1.089×10^{-2}	0.4839	4.105×10^{-3}	0.7937	1.078×10^{-2}	0.4843
256, 128	2.396×10^{-3}	0.8645	7.787×10^{-3}	0.5494	2.368×10^{-3}	0.8674	7.706×10^{-3}	0.5506
512, 256	1.316×10^{-3}	–	5.321×10^{-3}	–	1.298×10^{-3}	–	5.261×10^{-3}	–

Table 15. For Example 5.1, maximum point-wise errors $E^{N,M}$ and orders of convergence $Q^{N,M}$ when $\Lambda\varepsilon_1 < \vartheta\mu^2 < \Lambda\varepsilon_2$.

(N, M)	First Component z_1				Second Component z_2			
	BS mesh		S mesh		BS mesh		S mesh	
	$E^{N,M}$	$Q^{N,M}$	$E^{N,M}$	$Q^{N,M}$	$E^{N,M}$	$Q^{N,M}$	$E^{N,M}$	$Q^{N,M}$
32, 16	3.033×10^{-3}	0.7519	4.538×10^{-2}	0.5785	3.017×10^{-3}	0.7173	3.673×10^{-2}	0.5579
64, 32	1.801×10^{-3}	0.8302	3.039×10^{-2}	0.6617	1.835×10^{-3}	0.8317	2.495×10^{-2}	0.6564
128, 64	1.013×10^{-3}	0.8898	1.621×10^{-2}	0.7411	1.031×10^{-3}	0.8904	1.583×10^{-2}	0.7391
256, 128	5.467×10^{-4}	0.9147	9.698×10^{-3}	0.8211	5.562×10^{-4}	0.9149	9.484×10^{-3}	0.8322
512, 256	2.900×10^{-4}	–	5.489×10^{-3}	–	2.950×10^{-4}	–	5.327×10^{-3}	–

6. Conclusions

In this work, we have considered the efficient numerical resolution of a type of 2D parabolic singularly perturbed systems with two equations of convection-diffusion type. In the continuous problem, the parabolic partial differential equation contains small positive parameters on both the diffusion and the convection terms; moreover, we have assumed that the diffusion parameters can be distinct, having a very different order of magnitude between them, but the convection parameters are equal for both equations in the coupled system. Then, it is well known that, in general, different types of overlapping boundary layers appear on the outflow and the inflow boundary, which depend on the value and the ratio between the three small parameters. To solve the continuous problem, we have constructed a method that combines the classical implicit Euler method, to discretize in time on the most simple mesh (a uniform mesh), together with the well-known upwind finite difference scheme. It is defined on a special nonuniform mesh of BS type, which is considerably different to the standard piecewise uniform Shishkin mesh, in order to increase the order of uniform convergence. Therefore, we have proved that the fully discrete scheme is a uniformly convergent method; moreover, in the maximum norm, it has first order in both time and spatial variables, which is a better result than those in the literature, where the order of uniform convergence in space was usually almost first order due the logarithmic factor, which usually appears in the order of uniform convergence when standard Shishkin meshes are used. So, the numerical results obtained with our algorithm for some test problems are better than those in previous works in the literature, without any increase in the computational cost of the numerical algorithm; from them, we clearly can observe the overlapping layers in the numerical solution and also the important fact related with the order of uniform convergence. The numerical results showed are in agreement with the theoretical results proved in the work.

A. Proof of Lemma 4.3

A detailed analysis is presented for the layer function $\vec{\mathbf{w}}_l$, while a similar methodology can be extended to the remaining components. From the results established in Theorem 2.5, it follows that the truncation error corresponding to the singular component $\vec{\mathbf{w}}_l$ satisfies

$$\|\mathcal{L}^{N,N}_{\varepsilon,\mu}(\mathbf{W}_l - \mathbf{w}_l)\| \leq C\Big[\Delta t\Big\|\frac{\partial^2 \mathbf{w}_l}{\partial t^2}\Big\| + (h_i + h_{i+1})\Big(\boldsymbol{\varepsilon}\Big\|\frac{\partial^3 \vec{\mathbf{w}}_l}{\partial {x_1}^3}\Big\| + \boldsymbol{\mu}\Big\|\frac{\partial^2 \mathbf{w}_l}{\partial {x_1}^2}\Big\|\Big) + (k_j + k_{j+1})\Big(\boldsymbol{\varepsilon}\Big\|\frac{\partial^3 \mathbf{w}_l}{\partial {x_2}^3}\Big\| + \boldsymbol{\mu}\Big\|\frac{\partial^2 \mathbf{w}_l}{\partial x_2^2}\Big\|\Big)\Big]. \quad (A.1)$$

If $\tau_1 = \frac{1}{8}$, $\tau_2 = \frac{1}{4}$, and $\sigma_1 = \frac{1}{4}$, the proof can be readily obtained by applying standard techniques on uniform meshes, taking into account that it follows $\mu^{-1}\varepsilon_1 \leq CN^{-1}$, $\mu^{-1}\varepsilon_2 \leq CN^{-1}$, and $\mu \leq CN^{-1}$. Then, using Theorem 2.5, we have

$$|\mathcal{L}^{N,N}_{\varepsilon,\mu}(\boldsymbol{W}_l - \boldsymbol{w}_l)| \leq C\begin{pmatrix} N^{-1}\mu^3(\varepsilon_1^{-2}\mathcal{B}_1^l(x_{1i-1}) + \varepsilon_2^{-2}\mathcal{B}_2^l(x_{1i-1})) + \Delta t \\ N^{-1}\mu^3(\varepsilon_1^{-1}\varepsilon_2^{-1}\mathcal{B}_1^l(x_{1i-1}) + \varepsilon_2^{-2}\mathcal{B}_2^l(x_{1i-1})) + \Delta t \end{pmatrix}. \quad (A.2)$$

Now, define the mesh functions $\vec{\boldsymbol{\psi}}(x_{1i})$ and $\boldsymbol{\psi}(x_{2j})$ on $\overline{Q}^{N,M}$ by:

$$\psi_1(x_{1i}) = C\Big(\exp\Big(\frac{2h_i\mu}{\varepsilon_1}\Big)\frac{\varepsilon_1^{-1}\mu\Re_i}{N\ln N} + \exp\Big(\frac{2h_i\mu}{\varepsilon_2}\Big)\frac{\varepsilon_2^{-1}\mu\mathfrak{P}_i}{N\ln N}\Big) + C\Delta t, \quad (A.3a)$$

$$\psi_2(x_{1i}) = C\Big(\exp\Big(\frac{2h_i\mu}{\varepsilon_2}\Big)\frac{\varepsilon_1^{-1}\mu\ \mathfrak{P}_i}{N\ln N}\Big) + C\Delta t, \quad (A.3b)$$

where

$$\Re_i = \frac{\upsilon^{N-i} - 1}{\upsilon^N - 1},\ \text{with}\ \upsilon = 1 + \frac{\mu h_i}{\varepsilon_1},\ \mathfrak{P}_i = \frac{\lambda^{N-i} - 1}{\lambda^N - 1},\ \text{with}\ \lambda = 1 + \frac{\mu h_i}{\varepsilon_2}.$$

Similarly, the mesh function $\boldsymbol{\psi}(x_{2j})$ is defined along the x_2-direction.
Now, it follows directly that $0 \leq \Re_i$, and $\mathfrak{P}_i \leq 1$, and in addition,

$$(-\varepsilon_1\delta^2_{x_1x_1} + \mu D^-_{x_1})\Re_i = 0,\ (-\varepsilon_1\delta^2_{x_1x_1} + \mu D^-_{x_1})\mathfrak{P}_i = 0,$$

$$D^-_{x_1}\Re_i \leq \frac{\mu}{\varepsilon_1}\exp\Big(\frac{\mu x_{1i+1}}{\varepsilon_1}\Big),\ D^-_{x_1}\mathfrak{P}_i \leq \frac{\mu}{\varepsilon_2}\exp\Big(\frac{\mu x_{1i+1}}{\varepsilon_2}\Big).$$

Therefore, it is clear that we have

$$|\mathcal{L}^{N,N}_{\varepsilon,\mu}\boldsymbol{\psi}(x_{1i})| \leq \begin{pmatrix} C\frac{\varepsilon_1^{-2}\mu^3}{N\ln N}\mathcal{B}_1^l(x_{1i-1}) + C\frac{\varepsilon_2^{-2}\mu^3}{N\ln N}\mathcal{B}_2^l(x_{11i-1}) + C\Delta t \\ C\frac{\mu^3\varepsilon_1^{-1}\varepsilon_2^{-1}}{N\ln N}\mathcal{B}_2^l(x_{1i-1}) + C\Delta t \end{pmatrix}, \quad (A.4a)$$

and similarly, we can prove

$$|\mathcal{L}^{N,N}_{\varepsilon,\mu}\boldsymbol{\psi}(x_{2j})| \leq \begin{pmatrix} C\frac{\varepsilon_1^{-2}\mu^3}{N\ln N}\mathcal{B}_1^l(x_{2j-1}) + C\frac{\varepsilon_2^{-2}\mu^3}{N\ln N}\mathcal{B}_2^l(x_{2j-1}) + C\Delta t \\ C\frac{\mu^3\varepsilon_1^{-1}\varepsilon_2^{-1}}{N\ln N}\mathcal{B}_2^l(x_{2j-1}) + C\Delta t \end{pmatrix}. \quad (A.4b)$$

Then, defining the mesh function

$$\boldsymbol{\Psi}^{\pm}(x_{1i}, x_{2j}, t_k) = \boldsymbol{\psi}(x_{1i}) + \boldsymbol{\psi}(x_{2j}) \pm (\mathbf{W}_l - \mathbf{w}_l)(x_{1i}, x_{2j}, t_k),$$

it is straightforward to see that it holds

$$\boldsymbol{\Psi}^{\pm}(x_{1i}, x_{2j}, t_k) \geq \mathbf{0}, \quad (x_{1i}, x_{2j}, t_k) \in \Gamma^N \times (0, T],$$

and

$$\mathcal{L}^{N,N}_{\varepsilon,\mu}\mathbf{\Psi}^{\pm}(x_{1i}, x_{2j}, t_k) \geq \mathbf{0}, \quad (x_{1i}, x_{2j}, t_k) \in Q^{N,M},$$

where the above results follow from (A.2) and (A.4). Hence, by applying Lemma 3.1, we obtain

$$|(\mathbf{W}_l - \mathbf{w}_l)(x_{1i}, x_{2j}, t_k)| \leq C(N^{-1} + \Delta t).$$

Next, from (4.2), when $\tau_2 = \dfrac{\varepsilon_2}{\mu\vartheta}\ln N$, for the mesh points (x_{1i}, x_{2j}, t_k), $N/4 \leq i \leq N$, $0 \leq j \leq N$, and $0 \leq k \leq M$, we have

$$\begin{aligned} |(W_{l_1} - w_{l_1})(x_{1i}, x_{2j}, t_k)| &\leq |W_{l_1}(x_{1i}, x_{2j}, t_k)| + |w_{l_1}(x_{1i}, x_{2j}, t_k)| \leq C\mathcal{B}^{l,N}_2(x_{1i}) + C\mathcal{B}^{l,N}_2(x_{1i}) \\ &\leq C\mathcal{B}^{l,N}_2(\tau_2) + C\mathcal{B}^{l,N}_2(\tau_2) \leq CN^{-1}. \end{aligned} \tag{A.5}$$

Analogously, it follows that

$$|(W_{l_2} - w_{l_2})(x_{1i}, x_{2j}, t_k)| \leq CN^{-1}. \tag{A.6}$$

When $\tau_2 = \dfrac{\varepsilon_2}{\mu\vartheta}\ln N$, there are two distinct cases to consider: $2\varepsilon_1 \geq \varepsilon_2$ and $2\varepsilon_1 < \varepsilon_2$, respectively. In the case where $\dfrac{\varepsilon_2}{2} \leq \varepsilon_1 \leq \varepsilon_2$, for $N/8 \leq i \leq N/4$, $0 \leq j \leq N$, and $0 \leq k \leq M$, we observe that $\tau_2 \leq \dfrac{2\varepsilon_1}{\mu\vartheta}\ln N$ holds. Hence, we can obtain

$$|\mathcal{L}^{N,N}_{\varepsilon,\mu}(\mathbf{W}_l - \mathbf{w}_l)(x_{1i}, x_{2j}, t_k)| \leq C\begin{pmatrix} \varepsilon_1^{-1}\mu^2\mathcal{B}^l_1(x_{1i-1}) + \varepsilon_2^{-1}\mu^2\mathcal{B}^l_2(x_{1i-1}) + \Delta t \\ \varepsilon_2^{-1}\mu^2\mathcal{B}^l_2(x_{1i-1}) + \Delta t \end{pmatrix} \quad \left(\text{as } h_i \leq \frac{\varepsilon_1}{\mu}\right).$$

In the case $\varepsilon_2 > 2\varepsilon_1$, for $N/8 \leq i \leq N/4$, $0 \leq j \leq N$, and $0 \leq k \leq M$, we have

$$|\mathcal{L}^{N,N}_{\vec{\varepsilon},\mu}(\mathbf{W}_l - \mathbf{w}_l)(x_{1i}, x_{2j}, t_k)| \leq \begin{pmatrix} C\varepsilon_1^{-1}\mu^2\mathcal{B}^l_1(x_{1i-1}) + C\varepsilon_2^{-1}\mu^2\mathcal{B}^l_2(x_{1i-1}) + C\Delta t \\ C\varepsilon_2^{-1}\mu^2\mathcal{B}^l_1(x_{1i-1}) + C\varepsilon_2^{-1}\mu^2\mathcal{B}^l_2(x_{1i-1}) + C\Delta t \end{pmatrix}.$$

For $0 \leq i \leq \frac{N}{8}$, $0 \leq j \leq N$, $0 \leq k \leq M$, and $\tau_1 \leq \frac{\varepsilon_1}{\vartheta}\ln N$, the local error satisfies

$$|\mathcal{L}^{N,N}_{\varepsilon,\mu}(\mathbf{W}_l - \mathbf{w}_l)(x_{1i}, x_{2j}, t_k)| \leq C\begin{pmatrix} \varepsilon_1^{-1}\mu^2\mathcal{B}^l_1(x_{1i-1}) + \varepsilon_2^{-1}\mu^2\mathcal{B}^l_2(x_{1i-1}) + \Delta t \\ \varepsilon_2^{-1}\mu^2\mathcal{B}^l_2(x_{1i-1}) + \Delta t \end{pmatrix}.$$

For $0 \leq i \leq \dfrac{N}{8}$, $0 \leq j \leq N$, and $0 \leq k \leq M$, we define the mesh functions $\boldsymbol{\psi}(x_{1i})$ and $\boldsymbol{\psi}(x_{2j})$ by

$$\psi_1(x_{1i}) = C\left(\exp\left(\frac{2\vartheta h_i\mu}{\varepsilon_1}\right)\mathcal{B}^{l,N}_1(x_{1i}) + \exp\left(\frac{2\vartheta h_i\mu}{\varepsilon_2}\right)\mathcal{B}^{l,N}_2(x_{1i})\right) + C\frac{\mu\varepsilon^{-1}}{N\ln N}(\tau_2 - x_{1i}) + C\Delta t, \tag{A.7a}$$

$$\psi_2(x_{1i}) = C\left(\exp\left(\frac{2\vartheta h_i\mu}{\varepsilon_2}\right)\mathcal{B}^{l,N}_2(x_{1i})\right) + C\frac{\mu\varepsilon^{-1}}{N\ln N}(\tau_2 - x_{1i}) + C\Delta t. \tag{A.7b}$$

Similarly, the mesh function $\boldsymbol{\psi}(x_{2j})$ can be defined along the x_2-direction. Now, for $\frac{N}{8} \le i \le \frac{N}{4}$, $0 \le j \le N$, and $0 \le k \le M$, we consider the functions

$$\psi_1(x_{1i}) = C\Big(\mathcal{B}_1^{l,N}(x_{1i}) + \exp\Big(\frac{2\vartheta h_i\mu}{\varepsilon_2}\Big)\mathcal{B}_2^{l,N}(x_{1i})\Big) + C\frac{\mu\varepsilon^{-1}}{N\ln N}(\tau_2 - x_{1i}) + C\Delta t, \tag{A.7c}$$

$$\psi_2(x_{1i}) = C\Big(\exp\Big(\frac{2\vartheta h_i\mu}{\varepsilon_2}\Big)\mathcal{B}_2^{l,N}(x_{1i})\Big) + C\frac{\mu\varepsilon^{-1}}{N\ln N}(\tau_2 - x_{1i}) + C\Delta t. \tag{A.7d}$$

Analogously, the mesh function $\boldsymbol{\psi}(x_{2j})$ can be defined along the x_2-direction.

Now, we construct the barrier function

$$\boldsymbol{\Psi}^{\pm}(x_{1i}, x_{2j}, t_k) = \boldsymbol{\psi}(x_{1i}) + \boldsymbol{\psi}(x_{2j}) \pm (\mathbf{W}_l - \mathbf{w}_l)(x_{1i}, x_{2j}, t_k).$$

For $0 \le i \le \frac{N}{4}$, $0 \le j \le N$, and $0 \le k \le M$, it follows from Lemma 3.1 that

$$\boldsymbol{\Psi}^{\pm}(x_{1i}, x_{2j}, t_k) \ge \vec{\mathbf{0}}, \quad \text{for all} \quad 0 \le i \le \frac{N}{4},\ 0 \le j \le N,\ 0 \le k \le M.$$

Hence, it follows that

$$|(\mathbf{W}_l - \mathbf{w}_l)(x_{1i}, x_{2j}, t_k)| \le C(N^{-1} + \Delta t),\ \ 0 \le i \le N/4,\ 0 \le j \le N,\ 0 \le k \le M. \tag{A.8}$$

From (A.5), (A.6), and (A.8), for the case $\tau_2 = \frac{\varepsilon_2}{\mu\vartheta}\ln N$, it follows that

$$\left|(\mathbf{W}_l - \mathbf{w}_l)(x_{1i}, x_{2j}, t_k)\right| \le C(N^{-1} + \Delta t).$$

Next, the case $\tau_2 = 1/4$, $\sigma_1 = 1/4$, and $\tau_1 = \dfrac{\varepsilon_1}{\mu\vartheta}\ln N$ is considered; then, $\mu^{-1}\varepsilon_2 \le CN^{-1}$ holds for $(x_{1i}, x_{2j}, t_k) \in (0, \tau_1] \times (0, 1) \times (0, T]$, $h_i \le C\varepsilon_1\mu^{-1}$. Hence, from the truncation error estimate (4.4), we obtain

$$|\mathcal{L}_{\varepsilon,\mu}^{N,N}(\mathbf{W}_l - \mathbf{w}_l)(x_{1i}, x_{2j}, t_k)| \le C\begin{pmatrix}\varepsilon_1^{-1}\mu^2\mathcal{B}_1^l(x_{1i-1}) + \varepsilon_2^{-1}\mu^2\mathcal{B}_2^l(x_{1i-1}) + \Delta t\\ \varepsilon_2^{-1}\mu^2\mathcal{B}_2^l(x_{1i-1}) + \Delta t\end{pmatrix}.$$

For $(x_{1i}, x_{2j}, t_k) \in [\tau_1, \tau_2] \times (0, 1) \times (0, T]$, from (4.4) and Lemma 2.5, we have

$$|\mathcal{L}_{\varepsilon,\mu}^{N,N}(\mathbf{W}_l - \mathbf{w}_l)(x_{1i}, x_{2j}, t_k)| \le \begin{pmatrix}C\varepsilon_1^{-1}\mu^2\mathcal{B}_1^l(x_{1i-1}) + C\varepsilon_2^{-1}\mu^2\mathcal{B}_2^l(x_{1i-1}) + C\Delta t\\ C\varepsilon_2^{-1}\mu^2\mathcal{B}_2^l(x_{1i-1}) + C\varepsilon_2^{-1}\mu^2\mathcal{B}_2^l(x_{1i-1}) + C\Delta t\end{pmatrix}.$$

Similarly, for $(x_{1i}, x_{2j}, t_k) \in [\tau_2, 1) \times (0, 1) \times (0, T]$, from (4.4) and Lemma 2.5, we can obtain

$$|\mathcal{L}_{\varepsilon,\mu}^{N,N}(\mathbf{W}_l - \mathbf{w}_l)(x_{1i}, x_{2j}, t_k)| \le \begin{pmatrix}C\varepsilon_1^{-1}\mu^2\mathcal{B}_1^l(x_{1i-1}) + C\varepsilon_2^{-1}\mu^2\mathcal{B}_2^l(x_{1i-1}) + C\Delta t\\ C\varepsilon_2^{-1}\mu^2\mathcal{B}_2^l(x_{1i-1}) + C\varepsilon_2^{-1}\mu^2\mathcal{B}_2^l(x_{1i-1}) + C\Delta t\end{pmatrix}.$$

To analyze the layer component, an appropriate barrier function is introduced and defined by

$$\boldsymbol{\Psi}^{\pm}(x_{1i}, x_{2j}, t_k) = \boldsymbol{\psi}(x_{1i}) + \boldsymbol{\psi}(x_{2j}) \pm (\mathbf{W}_l - \mathbf{w}_l)(x_{1i}, x_{2j}, t_k) \text{ for } 0 \le i \le N/8,\ 0 \le j \le N,\ 0 \le k \le M,$$

where

$$\psi_1(x_{1i}) = C\Big(\exp\Big(\frac{2\vartheta h_i\mu}{\varepsilon_1}\Big)\mathcal{B}_1^{l,N}(x_{1i}) + \exp\Big(\frac{2\vartheta h_i\mu}{\varepsilon_2}\Big)\mathcal{B}_2^{l,N}(x_{1i})\Big) + C\frac{\mu\varepsilon^{-1}}{N\ln N}(\tau_1 - x_{1i}) + C\Delta t,$$

$$\psi_2(x_{1i}) = C\Big(\exp\Big(\frac{2\vartheta\vartheta h_i\mu}{\varepsilon_2}\Big)\mathcal{B}_2^{l,N}(x_{1i})\Big) + C\frac{\mu\varepsilon^{-1}}{N\ln N}(\tau_1 - x_{1i}) + C\Delta t,$$

for $N/8 \le i \le N/4,\ 0 \le j \le N,$ and $0 \le k \le M$, and as

$$\psi_1(x_{1i}) = C\mathcal{B}_1^{l,N}(x_{1i}) + C\exp\Big(\frac{2\vartheta h_i\mu}{\varepsilon_2}\Big)\mathcal{B}_2^{l,N}(x_{1i}) + C\frac{\mu\varepsilon^{-1}}{N\ln N}(\tau_2 - x_{1i}) + C\Delta t,$$

$$\psi_2(x_{1i}) = C\exp\Big(\frac{2\vartheta h_i\mu}{\varepsilon_2}\Big)\mathcal{B}_2^{l,N}(x_{1i}) + C\frac{\mu\varepsilon^{-1}}{N\ln N}(\tau_2 - x_{1i}) + C\Delta t,$$

and finally, for $N/4 \le i \le N,\ 0 \le j \le N,$ and $0 \le k \le M$, as

$$\psi_1(x_i) = C\mathcal{B}_1^{l,N}(x_{1i}) + CN^{-1}\exp\Big(\frac{2\vartheta h_i\mu}{\varepsilon_2}\Big)\mathcal{B}_2^{l,N}(x_{1i}) + C\Delta t,$$

$$\psi_2(x_{1i}) = C\mathcal{B}_1^{l,N}(x_{1i}) + CN^{-1}\exp\Big(\frac{2\vartheta h_i\mu}{\varepsilon_2}\Big)\mathcal{B}_2^{l,N}(x_{1i}) + C\Delta t.$$

Similarly, the mesh function $\vec{\boldsymbol{\psi}}(x_{2j})$ can be defined along the x_2-direction.

Hence, for all the considered cases, the following estimate is obtained:

$$\Big|(\mathbf{W}_l - \mathbf{w}_l)(x_{1i}, x_{2j}, t_k)\Big| \le C(N^{-1} + \Delta t),$$

which is the required result.

B. Proof of Lemma 4.4

If $\tau_1 = \dfrac{1}{8}$ and $\tau_2 = \dfrac{1}{4}$, the proof follows by applying standard techniques for uniform meshes, while taking into account that it holds $\mu^{-1}\varepsilon_1 \le CN^{-1}$, $\sqrt{\varepsilon_2} \le CN^{-1}$, and $\mu \le CN^{-1}$. Therefore, by utilizing (4.2) and Theorem 2.5, we obtain

$$\begin{aligned}\|\mathcal{L}_{\varepsilon,\mu}^{N,N}(\mathbf{W}_l - \mathbf{w}_l)\| &\le C\Big[\Delta t\Big\|\frac{\partial^2\mathbf{w}_l}{\partial t^2}\Big\| + (h_i + h_{i+1})\Big(\boldsymbol{\varepsilon}\Big\|\frac{\partial^3\mathbf{w}_l}{\partial {x_1}^3}\Big\| + \boldsymbol{\mu}\Big\|\frac{\partial^2\mathbf{w}_l}{\partial {x_1}^2}\Big\|\Big) + (k_j + k_{j+1})\Big(\boldsymbol{\varepsilon}\Big\|\frac{\partial^3\mathbf{w}_l}{\partial {x_2}^3}\Big\| + \boldsymbol{\mu}\Big\|\frac{\partial^2\mathbf{w}_l}{\partial {x_2}^2}\Big\|\Big)\Big]\\ &\le CN^{-1}.\end{aligned}$$

Further, if $\tau_1 = \dfrac{\varepsilon_1}{\mu\vartheta}\ln N$, $\tau_2 = \dfrac{1}{4}$, and $\sigma_1 = \dfrac{\tau_2}{2}$ and we assume that $(x_{1i}, x_{2j}, t_k) \in (\tau_2, 1-\tau_2) \times (0,1) \times (0,T] \cup (\tau_1, \tau_2) \times (0,1) \times (0,T] \cup (1-\tau_2, 1-\sigma_1) \times (0,1) \times (0,T]$, then we have

$$|\mathcal{L}_{\varepsilon,\mu}^{N,N}(\mathbf{W}_l - \mathbf{w}_l)(x_{1i}, x_{2j}, t_k)| \le C\begin{pmatrix} N^{-1}\varepsilon_2^{-1/2}\mathcal{B}_2^l(x_{1i-1}) + \Delta t\\ N^{-1}\varepsilon_2^{-1/2}\mathcal{B}_2^l(x_{1i-1}) + \Delta t\end{pmatrix}.$$

When $(x_{1i}, x_{2j}, t_k) \in (0, \tau_1] \times (0,1) \times (0,T]$ or $(x_{1i}, x_{2j}, t_k) \in [1-\sigma_1, 1] \times (0,1) \times (0,T]$, it follows that

$$|\mathcal{L}_{\varepsilon,\mu}^{N,N}(\mathbf{W}_l - \mathbf{w}_l)(x_{1i}, x_{2j}, t_k)| \leq C \begin{pmatrix} \mu^2\varepsilon_1^{-1} + \varepsilon_2^{-1/2} + \Delta t \\ \mu^2\varepsilon_1^{-1} + \varepsilon_2^{-1/2} + \Delta t \end{pmatrix} \left(\text{as } h_i \leq \frac{\varepsilon_1}{\mu}\right).$$

If $\tau_2 = \sqrt{\dfrac{\varepsilon_2}{\Lambda\vartheta}} \ln N$ and $\tau_1 = \dfrac{\tau_2}{2}$, with $\dfrac{\sqrt{\varepsilon_2}}{2} \leq \sqrt{\varepsilon_1} < \sqrt{\varepsilon_2}$, then $\tau_2 \leq C\sqrt{\varepsilon_1}\ln N$. To establish the error estimate in the region $(x_{1i}, x_{2j}, t_k) \in [\tau_2, 1-\tau_2] \times (0,1) \times (0,T]$, we construct suitable barrier functions

$$\mathcal{B}_1^{l,N}(x_{1i}) = \prod_{\iota=1}^{i}\left(1 + \left(\frac{\vartheta\mu}{2\varepsilon_1}\right)h_\iota\right)^{-1}, \quad \mathcal{B}_2^{l,N}(x_{1i}) = \prod_{\iota=1}^{i}\left(1 + \sqrt{\left(\frac{\Lambda}{\varepsilon_2}\right)}h_\iota\right)^{-1}, \tag{B.1}$$

with $\mathcal{B}_1^{l,N}(x_{10}) = \mathcal{B}_2^{l,N}(x_{10}) = 1$. After applying Theorem 2.5, we can conclude that it holds

$$|(\mathbf{W}_l - \mathbf{w}_l)(x_{1i}, x_{2j}, t_k)| \leq |\mathbf{W}_l(x_{1i}, x_{2j}, t_k)| + |\mathbf{w}_l(x_{1i}, x_{2j}, t_k)| \leq C\mathcal{B}_2^{l,N}(\tau_2) + C\mathcal{B}_2^{l,N}(\tau_2) \leq CN^{-1}.$$

To derive suitable error bounds in the regions $(x_{1i}, x_{2j}, t_k) \in (\tau_1, \tau_2) \times (0,1) \times (0,T]$ or $(1-\tau_2, 1-\sigma_1) \times (0,1) \times (0,T]$, using that $(h_i + h_{i+1}) \leq CN^{-1}$, $(k_j + k_{j+1}) \leq CN^{-1}$, it follows that

$$|\mathcal{L}_{\varepsilon,\mu}^{N,N}(\mathbf{W}_l - \mathbf{w}_l)(x_{1i}, x_{2j}, t_k)| \leq C \begin{pmatrix} N^{-1}\sqrt{\varepsilon_2}(\mu^3\varepsilon_1^{-2} + \varepsilon_2^{-1/2}) + \Delta t \\ N^{-1}\sqrt{\varepsilon_2}(\mu\varepsilon_1^{-1} + \varepsilon_2^{-1/2}) + \Delta t \end{pmatrix}.$$

Using the suitable barrier functions, then we have

$$|\mathcal{L}_{\varepsilon,\mu}^{N,N}(\mathbf{W}_l - \mathbf{w}_l)(x_{1i}, x_{2j}, t_k)| \leq C(N^{-1} + \Delta t).$$

For $(x_{1i}, x_2 j, t_k) \in (0, \tau_1) \times (0,1) \times (0,T]$ or $(1-\sigma_1, 1) \times (0,1) \times (0,T]$, the relation $h_i + h_{i+1} \leq CN^{-1}$ holds. Consequently, by applying the same arguments as before, the corresponding bounds follow.

Assuming $\tau_1 = \dfrac{\varepsilon_1}{\mu\vartheta}\ln N$ and $\tau_2 = \sqrt{\dfrac{\varepsilon_2}{\Lambda\vartheta}}\ln N$, in the regions $(x_{1i}, x_{2j}, t_k) \in [\tau_2, 1-\tau_2] \times (0,1) \times (0,T]$, $(0,\tau_1] \times (0,1) \times (0,T]$, or $(1-\sigma_1, 1) \times (0,1) \times (0,T]$, the desired bounds can be derived using similar arguments as those applied in the corresponding intervals of the previous cases. For the regions $(x_{1i}, x_{2j}, t_k) \in (\tau_1, \tau_2) \times (0,1) \times (0,T]$ or $(1-\tau_2, 1-\sigma_1) \times (0,1) \times (0,T]$, we have $h_i + h_{i+1} \leq CN^{-1}$. Consequently, we obtain

$$|\mathcal{L}_{\varepsilon,\mu}^{N,N}(\mathbf{W}_l - \mathbf{w}_l)(x_{1i}, x_{2j}, t_k)| \leq C(N^{-1} + \Delta t),$$

which is the required result.

Use of Generative-AI tools declaration

The authors declare they have not used Artificial Intelligence (AI) tools in the creation of this article.

Author contributions

Both authors are responsible of all sections and mathematical details in the manuscript; they wrote and reviewed the all manuscript. Ram Shiromani prepared the Figures and Tables included in the manuscript.

Acknowledgments

The research of the first author thanks to SCIT, Pune for financial support and the second author was partially supported by the project PID2022-136441NB-I00, the Aragón Government and the European Social Fund (group E24-17R).

Conflict of interest

The authors declare that they have no competing interests.

References

1. K. Aarthika, V. Shanthi, H. Ramos, A computational approach for a two-parameter singularly perturbed system of partial differential equations with discontinuous coefficients, *Appl. Math. Comput.*, **434** (2022), 127409. https://doi.org/10.1016/j.amc.2022.127409
2. D. Avijit, S. Natesan, SDFEM for singularly perturbed boundary-value problems with two parameters, *J. Appl. Math. Comput.*, **64** (2020), 591–614. https://doi.org/10.1007/s12190-020-01370-3
3. Z. Cen, Parameter-uniform finite difference scheme for a system of coupled singularly perturbed convection-diffusion equations, *J. Syst. Sci. Compl.*, **18** (2005), 498–510.
4. Y. Cheng, M. Peng, Y. Cheng, A hybrid interpolating element-free galerkin method for 3D steady-state convection diffusion problems, *Appl. Numer. Math.*, **208** (2025), 21–37. https://doi.org/10.1016/j.apnum.2024.09.024
5. C. Clavero, J. C. Jorge, An efficient numerical method for singularly perturbed time dependent parabolic 2D convection-diffusion systems, *J. Comput. Appl. Math.*, **354** (2019), 431–444. https://doi.org/10.1016/j.cam.2018.10.033
6. C. Clavero, J. C. Jorge, A splitting uniformly convergent method for one-dimensional parabolic singularly perturbed convection-diffusion systems, *Appl. Numer. Math.*, **183** (2023), 317–3323. https://doi.org/10.1016/j.apnum.2022.09.012
7. C. Clavero, J. C. Jorge, An efficient uniformly convergent method for multi-scaled two dimensional parabolic singularly perturbed systems of convection-diffusion type, *Appl. Numer. Math.*, **207** (2025), 174–192. https://doi.org/10.1016/j.apnum.2024.09.002
8. C. Clavero, R. Shiromani, An efficient numerical method for 2d elliptic singularly perturbed systems with different magnitude parameters in the diffusion and the convection terms, part II, *AIMS Math.*, **9** (2024), 35570–35598. https://doi.org/10.3934/math.20241688

9. C. Clavero, R. Shiromani, An efficient numerical method for 2D elliptic singularly perturbed systems with different magnitude parameters in the diffusion and the convection terms, *Comput. Math. Appl.*, **181** (2025), 287–322. https://doi.org/10.1016/j.camwa.2025.01.011

10. C. Clavero, R. Shiromani, V. Shanthi, A computational approach for 2d elliptic singularly perturbed weakly-coupled systems of convection-diffusion type with multiple scales and parameters in the diffusion and the convection terms, *Math. Meth. Appl. Sci.*, **47** (2024), 13510–13541. https://doi.org/10.1002/mma.10204

11. C. Clavero, R. Shiromani, V. Shanthi, A numerical approach for a two-parameter singularly perturbed weakly-coupled system of 2D elliptic convection-reaction-diffusion PDES, *J. Comput. Appl. Math.*, **436** (2024), 115422. https://doi.org/10.1016/j.cam.2023.115422

12. I. R. Epstein, L. Lengyel, S. Kádár, M. Kagan, M. Yokoyama, New systems for pattern formation studies, *Physica A: Stat. Mech. Appl.*, **188** (1992), 26–33.

13. P. l. Farrell, A. Hegarty, J. J. H. Miller, E. O'Riordan, G. I. Shishkin, Robust computational techniques for boundary layers, CRC Press (2000). https://doi.org/10.1201/9781482285727

14. M. Ghil, A. W. Robertson, Climate dynamics and predictability, *B. Am. Meteorol. Soc.*, **83** (2002), 571–591.

15. L. Govindarao, J. Mohapatra, S. R. Sahu, Uniformly convergent numerical method for singularly perturbed two parameter time delay parabolic problem, *Int. J. Appl. Comput. Math.*, **5** (2019). https://doi.org/10.1007/s40819–019–0672–5

16. L. Govindarao, S. R. Sahu, J. Mohapatra, Uniformly convergent numerical method for singularly perturbed two parameter time delay parabolic problem with two small parameters, *Iranian J. Sci. Tech., Transactions A: Sci.*, **43** (2019), 2373–2383. https://doi.org/10.1007/s40995-019-00697-2

17. A. Jha, M. K Kadalbajoo, A robust layer adapted difference method for singularly perturbed two-parameter parabolic problems, *Int. J. Comp. Math.*, **92** (2015), 204–1221.

18. Y. Kan-On, M. Mimura, Singular perturbation approach to a 3-component reaction-diffusion system arising in population dynamics, *SIAM J. Math. Anal.*, **29** (1998), 1519–15368. https://doi.org/10.1137/S0036141097318328

19. S. Kumar, M. Kumar, An efficient hybrid numerical method based on an additive scheme for solving coupled systems of singularly perturbed linear parabolic problems, *Math. Meth. Appl. Sci.*, **46** (2023), 1234–1256.

20. O. A. Ladyzhenskaya, N. N. Ural'tseva, Linear and quasilinear elliptic equations, Academic Press, New York (1968).

21. T. Linß, Layer-adapted meshes for reaction-convection-diffusion problems, Springer (2009).

22. L. B. Liu, G. Long, Y. Zhang, Parameter uniform numerical method for a system of two coupled singularly perturbed parabolic convection-diffusion equations, *Adv. Diff. Equat.*, **450** (2018). https://doi.org/10.1186/s13662–018–1907–13

23. J. D. Murray, Mathematical Biology I: An Introduction, Springer (2002). https://doi.org/10.1007/b98868

24. S. Nagarajan, A parameter robust fitted mesh finite difference method for a system of two reaction-convection-diffusion equations, *Appl. Num. Math.*, **179** (2022), 87–104. https://doi.org/10.1016/j.apnum.2022.04.017

25. E O'Riordan, M. L. Pickett, G. I. Shishkin, Numerical methods for singularly perturbed elliptic problems containing two perturbation parameters, *Math. Model. Anal.*, **11** (2006), 199–212. https://doi.org/10.3846/13926292.2006.9637313

26. E. O'Riordan, M. L. Pickett, A parameter-uniform numerical method for a singularly perturbed two parameter elliptic problem, *Adv. Comput. Math.*, **35** (2011), 57–82. https://doi.org/10.1007/s10444-010-9164-1

27. C. V. Pao, Nonlinear parabolic and elliptic equations, Plenum Press (1992). https://doi.org/10.1007/978-1-4615-3034-3

28. P. Peng, H. Cheng, Yumin Cheng, A hybrid reproducing kernel particle method for three-dimensional elasticity problems, *Int. J. Appl. Mech.*, **15** (2023), 2350080.

29. S. Priyadarshana, J. Mohapatra, An efficient computational technique for time dependent semilinear parabolic problems involving two small parameters, *J. Appl. Math. Comput.*, **69** (2023), 3721–3754. https://doi.org/10.1007/s12190-023-01900-9

30. S. Priyadarshana, J. Mohapatra, An efficient fractional step numerical algorithm for time-delayed singularly perturbed 2D convection-diffusion–reaction problem with two small parameters, *Numer. Algor.*, **97** (2024), 687–726. https://doi.org/10.1007/s11075-023-01720-9

31. S. Priyadarshana, J. Mohapatra, S. R. Pattaniak, Parameter uniform optimmal order numerical approximations for time-delayed parabolic convection diffusion problems involving two small parameters, *Comput. Appl. Math.*, **41** (2022). https://doi.org/10.1007/s40314–022–01928–w

32. R. M. Priyadharshini, N. Ramanujam, A. Tamilsevan, Hybrid difference schemes for a system of singularly perturbed convection-diffusion equations, *J. Appl. Math. Infor.*, **27** (2009), 1001–1015.

33. M. K. Singh, S. Natesan, Numerical analysis of singularly perturbed system of parabolic convection-diffusion problem with regular boundary layers, *Diff. Equat. Dyn. Syst.*, (2019). https://doi.org/10.1007/s12591–019–00462–2

34. M. K. Singh, S. Natesan, A robust computational method for singularly perurbed system of 2D parabolic convection-diffusion problems, *Int. J. Math. Model. Numer. Optim.*, **9** (2019), 127–1579.

35. M. K. Singh, S. Natesan, A parameter-uniform hybrid finite difference schme for singularly perturbed system of parabolic convection-diffusion problems, *Int. J. Comput. Math.*, **97** (2020), 875–903. https://doi.org/10.1080/00207160.2019.1597972

36. G. Zheng, Y. Cheng, The improved element-free galerkin method for diffusional drug release problems, *Int. J. Appl. Mech.anics*, **12** (2020), 2050096. https://doi.org/10.1142/S1758825120500969

AIMS Press